Supporting Information (SI):

Materials and Methods

Supplementary Text

Figures S1-S15

Datasets S1-S8

Supporting Information References

Materials and Methods

The vectors used in this study (SI Appendix, Dataset S5) were constructed using standard molecular cloning techniques, including restriction enzyme digestion, ligation, PCR, and Gibson assembly. Custom oligonucleotides were purchased from Integrated DNA Technologies. The vector constructs were transformed into *E. coli* strain *DH5α*, and 50 μg/ml of carbenicillin (Teknova) was used to isolate colonies harboring the constructs. DNA was extracted and purified using Plasmid Mini or Midi Kits (Qiagen). Sequences of the vector constructs were verified with Genewiz's DNA sequencing service. The constructs for CombiGEM-CRISPR are available to the academic community through Addgene.

To generate a lentiviral vector encoding an shRNA that targeted a specific gene, oligo pairs harboring the sense and antisense sequences were synthesized, annealed, and cloned in the AgeI- and EcoRI-digested pLKO.1 vector (1) (Addgene plasmid #10879) by ligation. The shRNA sense and antisense sequences were designed and constructed based on the siRNA Selection Program (http://sirna.wi.mit.edu/), and listed in SI Appendix, Dataset S6.

To create the pAWp30 lentiviral expression vector encoding Cas9 protein and Zeocin as the selection marker, EFS promoter and *Cas9* sequences were amplified from Addgene plasmid #49535, while the *Zeocin* sequence was amplified from Addgene plasmid #25736, by PCR using Phusion DNA polymerase (New England Biolabs). The PCR products were cloned into the pAWp11 lentiviral vector backbone using Gibson Assembly Master Mix (New England Biolabs).

To construct a storage vector containing U6 promoter (U6p)-driven expression of a sgRNA that targeted a specific gene, oligo pairs with the 20 bp gRNA target sequences were synthesized,

annealed, and cloned in the BbsI-digested pAWp28 vector using T4 ligase (New England Biolabs). To construct a lentiviral vector for U6p-driven expression of single or combinatorial gRNA(s), U6p-sgRNA expression cassettes were prepared from digestion of the storage vector with BglII and MfeI enzymes (Thermo Scientific), and inserted into the pAWp12 vector backbone or the sgRNA expression vector, respectively, using ligation via the compatible sticky ends generated by digestion of the vector with BamHI and EcoRI enzymes (Thermo Scientific). To express the gRNAs together with the dual RFP and GFP fluorescent protein reporters, the U6p-driven sgRNA expression cassettes were inserted into the pAWp9, instead of pAWp12, lentiviral vector backbone using the same strategy described above. The pAWp9 vector was modified from the pAWp7 vector backbone by introducing unique BamHI and EcoRI sites into the vector to enable the insertion of the U6p-sgRNA expression cassettes.

Assembly of the barcoded combinatorial sgRNA library pool

We built a library of 153 barcoded sgRNAs targeting a set of 50 genes encoding epigenetic regulators (3 sgRNAs per gene) and 3 control sgRNAs based on the publicly available GeCKOv2 library for genome-wide gene-knockout screening (2) (SI Appendix, Dataset S1). We scanned through the GeCKOv2 library, and found that only a small number (~2.8%) of the gRNAs in the library contained the four restriction sites (i.e., EcoRI, MfeI, BamHI, and BglII) used for CombiGEM assembly. Among the 6 sgRNAs per gene in the GeCKOv2 library, less than 1.8% and 0.15% of genes have more than one and two of their sgRNAs, respectively, that contain any of these four restriction sites. In the library used in this study, only one sgRNA (i.e. PRMT3-sg3) contained an EcoRI recognition site. Our CombiGEM method is therefore compatible with existing gRNA libraries design for conducting large-scale screening experiments. Other restriction enzyme pairs that have compatible ends can also be used to assemble combinatorial gRNA expression vectors with CombiGEM.

An array of 153 oligo pairs (Oligo F-(x) and Oligo R-(x), where x = 1 to 153) harboring the barcoded gRNA sequences were synthesized, and annealed to create double-stranded inserts harboring the 20 bp gRNA target sequences, two BbsI restriction sites, 8 bp barcodes unique to each sgRNA while differed from each other by at least two bases, and 5’ overhangs at their ends. To generate the pooled storage vector library, the 153 annealed inserts were mixed at equal ratios

and cloned in the pAWp28 storage vector (digested with BbsI and MfeI) via a single pot of ligation reaction via their compatible ends. To build the barcoded sgRNA library, another one-pot ligation reaction was performed with the pooled storage vector library digested with BbsI, and an insert containing the gRNA scaffold sequence, BamHI and EcoRI restriction sites, and 5' overhangs at their ends that was prepared via synthesis and annealing of an oligo pair S1 and S2. The sequences of oligo S1 and S2 were 5'-GTTTTAGAGCTAGAAATAGCAAGTTAAAATAAGGCTAGTCCGTTATCAACTTGAAAAAGTGGCACCGAGTCGGTGCTTTTTTGGATCCGCAACGGA-3' and 5'-GAATTCCGTTGCGGATCCAAAAAAGCACCGACTCGGTGCCACTTTTTCAAGTTGATAACGGACTAGCCTTATTTTAACTTGCTATTTCTAGCTCTA-3', respectively. The pooled storage vector and the barcoded sgRNA libraries were both prepared in Endura competent cells (Lucigen) and purified by the Plasmid Midi Kit (Qiagen). We confirmed that 97% (i.e., 32/33 *E. coli* colonies) of randomly picked colonies from the barcoded sgRNA storage pool harbored the correct gRNA target sequences via Sanger sequencing.

Pooled lentiviral vector libraries harboring single or combinatorial gRNA(s) were constructed with same strategy as for the generation of single and combinatorial sgRNA constructs described above, except that the assembly was performed with pooled inserts and vectors, instead of individual ones. Briefly, the pooled U6p-sgRNA inserts were generated by a single-pot digestion of the pooled storage vector library with BglII and MfeI. The destination lentiviral vector (pAWp12) was digested with BamHI and EcoRI. The digested inserts and vectors were ligated via their compatible ends (i.e., BamHI + BglII & EcoRI + MfeI) to create the pooled one-wise sgRNA library (153 sgRNAs) in lentiviral vector. The one-wise sgRNA vector library was digested again with BamHI and EcoRI, and ligated with the same U6p-sgRNA insert pool to assemble the two-wise sgRNA library (153 x 153 sgRNAs = 23,409 total combinations). After the pooled assembly steps, the sgRNAs were localized to one end of the vector construct and their respective barcodes were concatenated at the other end. The lentiviral sgRNA library pools were prepared in XL10-Gold ultracompetent cells (Agilent Technologies) and purified by Plasmid Midi Kit (Qiagen). Sanger sequencing analysis revealed that the majority of *E. coli* colonies with the assembled barcoded sgRNA constructs harbored the expected gRNA target sequences in both the one-wise (i.e., 8/8 colonies) and the two-wise (i.e., 15/18 colonies)

lentiviral vector libraries.

Cell culture

HEK293T, MDA-MB-231, and BxPC-3 cells were obtained from ATCC. OVCAR8-ADR cells were a gift from T. Ochiya (Japanese National Cancer Center Research Institute, Japan). The identity of the OVCAR8-ADR cells was authenticated (Genetica DNA Laboratories). OVCAR8-ADR, MDA-MB-231, and BxPC-3 cells stably expressing Cas9 protein (i.e., OVCAR-ADR-Cas9, MDA-MB-231-Cas9, and BxPC-3-Cas9 cells) were generated by lentiviral infection of their parental cells with the pAWp30 vector and selected for three weeks with Zeocin (Life Technologies) at 50 μg/ml (for BxPC-3-Cas9 cells) or 200 μg/ml (for OVCAR-ADR-Cas9 and MDA-MB-231-Cas9 cells). HEK293T cells were cultured in DMEM supplemented with 10% heat-inactivated fetal bovine serum and 1X antibiotic-antimycotic (Life Technologies) at 37^{o}C with 5% CO_2. OVCAR8-ADR, MDA-MB-231, BxPC-3, and their respective Cas9-expressing cells were cultured in RPMI supplemented with 10% heat-inactivated fetal bovine serum and 1X antibiotic-antimycotic at 37^{o}C with 5% CO_2. For drug treatment, SD70 (Xcessbio #M60194), GSK-J4 (Cayman Chemical #12073), and/or (+)-JQ1 (Cayman Chemical #11187) were used to treat OVCAR8-ADR cells at indicated drug doses prior to the cell viability assays.

Lentivirus production and transduction

Lentiviruses were produced and packaged in HEK293T cells in 6-well format. HEK293T cells were maintained at ~70% confluency before transfection. FuGENE HD transfection reagents (Promega) were mixed with 0.5 μg of lentiviral vector, 1 μg of pCMV-dR8.2-dvpr vector, and 0.5 μg of pCMV-VSV-G vector in 100 μl of OptiMEM medium (Life Technologies), and were incubated for 15 minutes at room temperature before adding to cell culture. Culture medium was replaced the next day. Supernatant containing newly produced viruses were collected at 48-hour and 96-hour post-transfection, and filtered through a 0.45 μm polyethersulfone membrane (Pall). Filtered viral supernatant was used to infect cells in the presence of 8 μg/ml polybrene (Sigma) overnight for transduction with individual vector constructs. For pooled lentiviral library production used in the screens, lentivirus production and transduction were scaled up using the same experimental procedures. Filtered viral supernatant was concentrated using Amicon Ultra Centrifugal Filter Unit (Millipore). Cells were infected in the presence of 8 μg/ml polybrene at a

multiplicity of infection of about 0.3 to 0.5 to ensure single copy integration in most cells, which corresponded to an infection efficiency of 30-40%. The total number of cells used in the screening was approximately 300-fold more than the library size in order to maintain library coverage and reduce any spurious effects due to random lentiviral integration into the genome. Cell culture medium was replaced the next day after infection and cultured for indicated time periods prior to experiments.

Sample preparation for barcode sequencing

To prepare samples from cultured cells for barcode sequencing, genomic DNA was extracted and prepared using DNeasy Blood & Tissue Kit (Qiagen) according to the manufacturer's protocol. For the barcoded sgRNA plasmid libraries, plasmid DNA transformed into *E. coli* was extracted using the Plasmid Midi Kit (Qiagen). DNA concentrations were determined using Quant-iT PicoGreen dsDNA Assay Kit (Life Technologies).

A ~360 bp fragment containing unique barcode representing each combination within the pooled vector and infected cell libraries was PCR amplified from the plasmid/genomic DNA samples using KAPA HiFi Hotstart Ready Mix (Kapa Biosystems). For plasmid DNA, 1 ng of DNA template was added for a 25-µl PCR reaction. For genomic DNA, 800 ng of DNA was added for a 50-µl PCR reaction and a total of 64 PCR reactions were performed for each genomic DNA sample to ensure that the number of cell genomes being amplified was more than 100 times the library size. Moreover, the PCR parameters were optimized to ensure that PCR amplification steps were maintained in the exponential phase to avoid PCR bias. The Illumina anchor sequences and an 8 base-pair indexing barcode were added during the PCR for multiplexed sequencing. The primer pair sequences used to amplify barcode sequence were 5'-AATGATACGGCGACCACCGAGATCTACACGGATCCGCAACGGAATTC-3'
and 5'-
CAAGCAGAAGACGGCATACGAGATNNNNNNNNGGTTGCGTCAGCAAACACAG-3', where NNNNNNNN indicates a specific indexing barcode assigned for each experimental sample.

The PCR products containing the barcode sequences were then purified based on fragment size

by running on a 1.5% agarose gel and further extracted using the QIAquick Gel Extraction Kit (Qiagen). The PCR product concentrations were determined by quantitative PCR using KAPA SYBR Fast qPCR Master Mix (Kapa Biosystems) and the Illumina Library Quantification Kit (Kapa Biosystems). The forward and reverse primer used for quantitative PCR were 5'-AATGATACGGCGACCACCGA-3' and 5'-CAAGCAGAAGACGGCATACGA-3' respectively. The PCR products from different samples were then pooled at a desired ratio for multiplexed sample sequencing and loaded on the Illumina HiSeq system with CombiGEM barcode primer (5'-CCACCGAGATCTACACGGATCCGCAACGGAATTC-3')
and indexing barcode primer
(5'-GTGGCGTGGTGTGCACTGTGTTTGCTGACGCAACC-3').

Barcode sequencing data analysis

Barcode reads for each gRNA combinations were processed from the Illumina sequencing data. Each sample was categorized by the indexing barcodes. The barcoded gRNA combinations were relatively evenly distributed in the libraries, with the majority of the barcoded sgRNAs (i.e., 96.7% in the one-wise plasmid pool; 89.4% and 92.3% in the two-wise plasmid and the 5-day post-infected cell pools, respectively) detected within a 5-fold range from the mean barcode reads per combination (SI Appendix, Fig. S3*A*, *B*). Less than 5.8% and 4.2% of the gRNA combinations were covered by <100 reads in the two-wise plasmid and infected cell pools, respectively (SI Appendix, Fig. S3*A*, *B*).

In the pooled screen, we correlated the proliferation rate of a particular clone based on the relative frequency of its barcode with regard to the whole population. Barcode reads representing each combination were normalized per million reads for each sample. As measures of cell proliferation, barcode count ratios of normalized barcode reads comparing day 20 against day 15 groups were calculated as fold changes. Pro-proliferation and anti-proliferation phenotypes had fold changes of normalized barcode reads of > 1 and < 1 respectively, while no phenotypic change resulted in a fold change = 1. Barcodes that gave less than ~100 absolute reads in the day 15 group were filtered out to improve data reliability. Data variability could be further reduced by increasing the fold representation of cells per combination in the pooled screen (3). The fold changes of the different possible orders of each same gRNA combination were averaged, and a

coefficient of variation (CV) of < 0.2 and < 0.4 was observed for over 82% and 95% of the combinations, respectively (SI Appendix, Fig. S8). The calculated fold change was log transformed to give the $\log_2$ ratio. Screens were performed in two biological replicates with independent infections of the same lentiviral libraries. Combinations were ranked by the $\log_2$ ratio across all experimental conditions. We defined the set of top hits based on two criteria: 1) $\log_2$ ratios that were less than -0.90 (i.e., at least three standard deviations from the mean of gRNA combinations harboring only the control sgRNAs that are highlighted in orange in Fig. 2*B* and SI Appendix, Fig. S9) in both biological replicates, and 2) recovered at a low false-discovery rate (FDR). The P-value for the $\log_2$ ratio of each combination was computed by comparing the $\log_2$ ratio with those contained within the whole population obtained from the two replicates using the two-sample, two-tailed Student's t-test (MATLAB function 'ttest2'). The distribution of the $\log_2$ ratios is shown in SI Appendix, Fig. S9*B*. The adjusted P-values (i.e., Q-values) were calculated based on the distribution of P-values (MATLAB function 'mafdr'(4)) to correct for multiple hypothesis testing. A $\log_2$ ratio was considered as statistically significant relative to the entire population based on a Q-value cutoff at <0.01. The list of two-wise gRNA hits are shown in SI Appendix, Dataset S4, and are highlighted in blue in Fig. 2*B* and SI Appendix, Fig. S9*A, C*. For further analysis, our screen data are included in SI Appendix, Datasets S7 and S8.

Cell viability assay

The MTT colormetric assay was performed to assess cell viability. For each 96 well, 100 µl of MTT (3-(4,5-dimethylthiazol-2-yl)-2,5-diphenyltetrazolium bromide) solution (Sigma) was added to the cell cultures. Cells were incubated for 3 hours at 37^{o}C with 5% CO_2. Viable cells convert the soluble MTT salt to insoluble blue formazan crystals. Formazan crystals were dissolved with 100 µl of solubilization buffer at 37^{o}C. Absorbance reading at an optical density (OD) of 570nm and 650nm (reference) were measured using a Synergy H1 Microplate Reader (BioTek).

Drug synergy quantification

The Bliss independence (BI) model (5) and the Highest Single Agent (HSA) model (6) are commonly used methods to evaluate synergy between drug combinations.

Based on the BI model, the expected effect (E_{Exp}) is given by:

$E_{Exp} = E_A + E_B – (E_A \times E_B)$,

where E_A is the growth inhibition effect observed at a certain concentration of drug A alone, and E_B is the growth inhibition effect observed at a certain concentration of drug B alone. E_{Obs} is the observed growth inhibition effect for the drug combination (A + B), each at the same concentration as in E_A and E_B, respectively. Each effect is expressed as a fractional inhibition between 0 and 1. When $E_{Obs} – E_{Exp} > 0$, the two drugs are considered to be interacting synergistically.

The HSA model is similar to the BI model except, according to the HSA model, E_{Exp} is equal to the larger of the growth inhibition effect produced by the combination's single drug agents (E_A or E_B) at the same concentrations as in the drug combination (A + B).

We considered two drugs to be synergistic if $E_{Obs} – E_{Exp} > 0.1$ (i.e. > 10% of excess inhibition over the predicted BI and HSA models in Fig. 3*C, D*) for at least two different concentration combinations in both models to enhance the stringency of our criteria.

Flow cytometry

Cells were collected at 4-day and 8-day post infection. Samples were washed and resuspended in 1x PBS supplemented with 2% fetal bovine serum. To remove any clumps of cells, the resuspended cells were passed through cell strainers before loading onto the LSRII Fortessa flow cytometer (Becton Dickinson). At least 20,000 events were acquired per sample. Proper laser sets and filters were selected based on cell samples. Forward scatter and side scatter were used to identify appropriate cell populations. Data were analyzed using the manufacturer's built-in software.

Fluorescence microscopy

Cultured cell were directly observed under an inverted fluorescent microscope (Zeiss) three days post-lentiviral infection. Images were captured using the Zeiss built-in software.

Quantitative PCR (qRT-PCR)

RNA extraction and qRT-PCR were performed as described previously (7). Primers used are listed in SI Appendix, Dataset S2.

Immunoblot analysis

Cells were lysed in 2X RIPA buffer supplemented with protease inhibitors. Lysates were homogenized using a pestle motor mixer (Agros) for 30 seconds, and then centrifuged at 15,000 rpm for 15 min at 4^{o}C. Supernatants were quantified using the BCA assay (Thermo Scientific). Protein was denatured at 99^{o}C for 5 minutes before gel electrophoresis on a 4-15% polyacrylamide gel (Bio-Rad). Proteins were transferred to nitrocellulose membranes at 80V for 2 hours at 4^{o}C. Primary antibodies used were: anti-BRD4 (1:2,000, Cell Signaling #13440), anti-KDM4C (1:1,000, Abcam ab85454) anti-KDM6B (1:1,000, Abcam ab85392), and anti-beta-actin (1:4,000, Abcam ab6276). Secondary antibodies used were: HRP-linked anti-rabbit IgG (1:2,000, Cell Signaling #7074), and HRP-linked anti-mouse IgG (1:4,000, Cell Signaling #7076). Membranes were developed by SuperSignal West Pico chemiluminescent substrate (Thermo Scientific) and imaged using a ChemiDoc Touch imaging system (BioRad).

Surveyor assay

The Surveyor assay was carried out to evaluate DNA mismatch cleavage at genomic loci targeted by the gRNAs. Genomic DNA was extracted from cell cultures using QuickExtract DNA extraction solution (Epicentre) according to the manufacturer's protocol. Amplicons harboring the targeted loci were generated by PCR using Phusion DNA polymerase and primers listed in SI Appendix, Dataset S9. About 200 ng of the PCR amplicons were denatured, self-annealed, and incubated with 1.5 µl of Surveyor Nuclease (Transgenomic) at 42^{o}C for 30 minutes. The samples were then analyzed on a 2% agarose gel. The expected uncleaved and cleaved bands for the targeted alleles studied in this work are listed in SI Appendix, Fig. S4.

Sequencing analysis for indel detection

Deep sequencing was performed to measure indel generation efficiency at genomic loci targeted by the gRNAs. Genomic DNA was extracted from cell cultures using DNeasy Blood & Tissue

Kit (Qiagen) according to the manufacturer's protocol. 66 ng of genomic DNA isolated from ~10,000 OVCAR8-ADR-Cas9 cells harboring the gRNA expression construct was used as the template for the first round of PCR using Phusion DNA polymerase and primers listed in SI Appendix, Dataset S10 to amplify each of the on-target and off-target loci and add priming sequences for the second round of PCR. Potential off-target loci were identified for individual gRNAs using the CRISPR design (8) (http://tools.genome-engineering.org) and CCTop (9) (http://crispr.cos.uni-heidelberg.de) prediction tools. The ~250 bp PCR product was purified using QIAquick PCR Purification Kit (Qiagen). 1 ng of the purified PCR product was then used as the template for the second round of PCR using Phusion DNA polymerase. The Illumina anchor sequences and a 6 base-pair indexing barcode were added during the second round of PCR for multiplexed sequencing. The primer pair sequences were 5'-AATGATACGGCGACCACCGAGATCTACACTCTTTCCCTACACGACGCTCTTCCGATCT-3' and 5'-CAAGCAGAAGACGGCATACGAGATNNNNNNGTGACTGGAGTTCAGACGTGTGCTCTTCCG-3', where NNNNNN indicates a specific indexing barcode assigned for each experimental sample. The ~300 bp PCR amplicon was then purified based on fragment size by running on a 1.5% agarose gel and extracted using the QIAquick Gel Extraction Kit (Qiagen). The purified PCR amplicons from each experimental sample were pooled at a 1:1 ratio, and loaded on the Illumina MiSeq system for paired-end sequencing. The paired-end read primers were 5'-ACACTCTTTCCCTACACGACGCTCTTCCGATCT-3' and 5'-GTGACTGGAGTTCAGACGTGTGCTCTTCCGATCT -3', and the indexing barcode primer was 5'-AGATCGGAAGAGCACACGTCTGAACTCCAGTCAC-3'. Sequencing data was demultiplexed using the indexing barcodes, aligned to the reference amplicon sequences obtained from uninfected OVCAR8-ADR-Cas9 cells, and analyzed for indels. More than 4.2 million reads per sample were used to evaluate the genomic diversity of the ~10,000 cells. Indel generation preference was evaluated by plotting the frequency of indel sizes for a given locus. The sequence alignment for the barcoded reads was performed using a custom written C++ code implementing the Needleman-Wunsch algorithm. Indel frequency calculation and plotting was performed on Matlab.

Sanger sequencing was performed to analyze the genome modifications generated by the

expression of combinatorial gRNAs in single-cell-derived clones. Cells infected with the combinatorial gRNA constructs were cultured for 12 days, and re-plated in 96-well plates as single cells by serial dilution of the cultures. Genomic DNA was extracted from the isolated single cell-expanded clones after culturing for 5 to 21 days using QuickExtract DNA extraction solution, and amplicons harboring the targeted alleles were prepared by PCR using Phusion DNA polymerase and primers listed in SI Appendix, Dataset S9. The PCR amplicons were cloned into a TOPO vector using TA Cloning Kit (Life Technologies) according to the manufacturer's protocol, and the nucleotide mutations, insertions, and deletions were identified using Sanger sequencing.

To analyze indel generation by the expression of combinatorial gRNAs at the single-cell level, targeted allele sequencing was performed on whole genome-amplified DNA from individual cells. OVCAR8-ADR-Cas9 cells harboring combinatorial gRNA expression constructs were cultured for 19 days, and sorted into 96-well plates as single cells using a FACSAria sorter (Becton Dickinson). Whole genome amplification (WGA) was then performed using the REPLI-g Single Cell Kit (Qiagen) according to the manufacturer's recommendations. Next, PCR enrichment of the targeted genomic loci was performed using KAPA HiFi Hotstart Ready Mix and primers listed in SI Appendix, Dataset S11. An Exonuclease I (New England Biolabs) digest was performed at 37^{o}C for 1 hour to remove excess primers and then a second round of PCR was performed to add sequencing adaptors and unique index barcodes to each sample. The latter primer sequences were 5'-CAAGCAGAAGACGGCATACGAGATNNNNNNNNGTCTCGTGGGCTCGGAGATGTGTATAAGAGACAG -3' (N7XX) and 5'-AATGATACGGCGACCACCGAGATCTACACNNNNNNNNTCGTCGGCAGCGTCAGATGTGTATAAGAGACAG -3' (N5XX), where NNNNNNNN indicates a specific index barcode assigned for each well. To prepare the sequencing library, 5 µl of PCR product from each well was pooled in a 1.5 ml microcentrifuge tube. The total volume was measured, and 0.9 volumes of Agencourt AMPure XP SPRI beads (Beckman Coulter) were added. After mixing, the bead suspension was incubated for 5 minutes at room temperature and then placed on a DynaMag-2 magnet for 5 minutes. The supernatant was removed and the beads were washed twice with 500 µl of 80% ethanol. After drying, DNA was eluted from the beads with 30 µl of TE buffer. A

reverse SPRI was then performed to remove the larger-sized DNA fragments: here, 0.5 volumes of SPRI beads was added to the eluent, and, after mixing, the supernatant was transferred to a new 1.5 ml microcentrifuge tube. At this point, one volume of SPRI beads was then added to the supernatant, the sample was mixed, and, after separation with a magnet, the beads were rinsed twice with 80% ethanol and air-dried before collecting the eluent in 30 µl of TE buffer. The purified library was then sequenced on an Illumina MiSeq instrument using a 300-cycle v3 kit (pair-end read: 200 bp for read 1, 100 bp for read 2). Sequencing reads were demultiplexed for each cell based on the barcodes. The sequences in each cell were counted and were aligned against the reference wild-type sequences to determine the frequency of single- and dual- gene edited cells.

RNA-Seq and data analysis

RNA was extracted from cells using TRIzol Plus RNA Purification Kit (Life Technologies) according to the manufacturer's protocol and treated with PureLink on-column DNase kit (Life Technologies). RNA quality and concentration was determined using NanoDrop Spectrophotometer. RNA samples were reverse-transcribed using SuperScript III Reverse Transcriptase (Life Technologies), Random Primer Mix (New England Biolabs) and RNAse OUT (Invitrogen). Sequencing libraries were prepared using the Illumina Library Prep Kit, starting with an input amount of 1 µg total RNA and following the manufacturer's recommendations. After PCR amplification, the libraries were size-selected to 300 +/- 25 bp on a 2% agarose gel (E-Gel EX, Invitrogen) and submitted to single-end sequencing on an Illumina HiSeq 2000 instrument. RNA-Seq experiments were performed in two biological replicates.

Raw single-end reads of the cDNA fragments were aligned to the human transcriptome (RefSeq, hg19) using TopHat2 (10) and Bowtie (11). Differentially expressed genes between samples were called using Cuffdiff2 (12) with the bias correction option, masking reads mapping to mitochondrial and ribosomal RNA transcripts. Genes were called differentially expressed if they met a minimum of 0.1 fragments per kilobase per million reads (FPKM) in at least one of the conditions tested, the absolute $\log_2$-fold-change was at least 0.5, and the P-value after multiple hypothesis correction (Q-value) was less than 0.05. Gene set enrichment analysis was performed using MSigDB database (http://www.broadinstitute.org/gsea/index.jsp) (13). All RNA-Seq data

has been deposited in the Gene Expression Omnibus (GEO) database (www.ncbi.nlm.nih.gov/geo; accession no. GSE71074).

Mathematical modeling of cell proliferation in a mixed population

To estimate how different parameters affect results in our pooled screens, we simulated cell proliferation in a mixed cell population harboring gRNA combinations that exhibit different growth rates. At a given time (t), the total cell count (C_N) in the population is represented by the summation of individual cell counts containing different combinations (C_i; 1 to N, where N is the total number of combinations), such that $C_N(t) = \sum_{i=1}^{N} C_i(t)$.

For each individual gRNA combination, cell growth is represented by Eq. (1). Based on an exponential cell growth model, cells with each gRNA combination consist of two populations: one with a modified growth rate (k_m) due to gene disruption by the CRISPR-Cas9 system, and the other (unmodified cells) with the wild-type growth rate (k_{wt}). The former population is defined as a fraction of cells, p, which is limited by the cleavage efficiency of the CRISPR-Cas9 system. For simplicity, we assumed that p was constant throughout the duration of the assay.

$$C_i(t) = p\ C_i(t) + (1-p)C_i(t) = \ pC_0e^{k_m t} + (1-p)C_0e^{k_{wt}t} \qquad \text{(Eq. 1)}$$

where p represents the fraction of mutated cells with a modified growth rate, and C_0 represents the initial number of cells carrying the same barcoded gRNA combination. The cell growth rate (k) is evaluated from the cell's doubling time ($T_{doubling}$) following Eq. 2. The doubling time for wild-type OVCAR8-ADR-Cas9 cells was experimentally determined to be ~24 hours (data not shown).

$$k = \ln 2\ /\ T_{doubling} \qquad \text{(Eq. 2)}$$

For simplicity in modeling, we segregated the total cell population into three sub-populations with different growth phenotypes as described in Eq. (3).

$$C_N(t) = \sum_{i=1}^{N} C_i(t) \approx f_{wt}N \times C_0 e^{k_{wt}t} + f_s N \times C_{i,slow}(t) + f_f N \times C_{i,fast}(t) \quad \text{(Eq. 3)}$$

where $C_{i,slow}(t)$ and $C_{i,fast}(t)$ represent the average growth profiles of cells with anti-proliferative gRNAs and pro-proliferative gRNAs, respectively, which are determined by Eq. (1). At the start of the experiment, the percentages of the overall population that behave as wild type or that contain anti-proliferative gRNAs and pro-proliferative gRNAs are represented by f_{wt}, f_s and f_f, respectively.

Based on this mixed cell growth model, we modeled the relative frequency (*R. F.*) of a pro-proliferative gRNA's and an anti-proliferative gRNA's representation in the whole population. The relative frequency is defined as the barcode abundance at a given time compared to the initial time point (i. e., $R.F. = \frac{F(t)}{F(t=0)}, where\ F = C_i(t)/C_N(t)$). The total number of combinations in a pool, N and the initial number of cells, C_0, do not impact the relative frequency results. After running the simulation with defined parameters, we observed enrichment and depletion of a pro-proliferative gRNA and anti-proliferative gRNA in the population, respectively (SI Appendix, Fig. S7*A*). The degree of enrichment and depletion was observed to change with different percentages (i.e., 2, 5, or 10%) of initial gRNA combinations defined to have an anti-proliferative (f_s) and pro-proliferative (f_f) response (SI Appendix, Fig. S7*A*). We further evaluated the relative frequency of an anti-proliferative gRNA's representation by modulating the doubling time of modified cells ($T_{doubling,m}$) and the fraction of cells with the modified growth rate (p) for the anti-proliferative gRNA. Assuming that p stayed constant throughout the experiment, the representation of an anti-proliferative clone in the entire cell population could be depleted by ~23% to 97% under the parameter ranges shown in SI Appendix, Fig. S7*B, C*. This model represents a simplified version of cell growth dynamics by segregating cell populations into sub-populations with average growth rates and does not account for potential interactions between cells. Based on our model, the sensitivity of our screen could be enhanced with improved gRNA efficiencies to increase the fraction of cells with modified growth rates and by increasing the assay time.

Supplementary Text

Author Contributions

A.S.L.W., G.C.G.C., and T.K.L. conceived the work. A.S.L.W., G.C.G.C., C.H.C., and T.K.L. designed and performed the experiments with help from all authors. A.S.L.W., G.C.G.C., and T.K.L. designed and developed the combinatorial genetic screening pipeline. A.S.L.W., G.C.G.C., and C.H.C. performed the combinatorial genetic screening, computational analyses on the screen data, and validation experiments. G.C.G.C. and A.S.L.W. performed the drug synergy experiments. A.S.L.W., C.H.C., S.D.P., and M.H. performed deep sequencing and analyzed CRISPR on- and off-targeting effects. A.S.L.W. and G.C.G.C. performed the targeted sequencing of single-cell-derived clones. C.H.C., S.W.K., A.G., A.S.L.W., and A.K.S. performed the single-cell WGA analysis. G.C.G.C., G.P., P.M., M.A., A.S.L.W., and E.F. performed the RNA-Seq experiments and analyzed the data. C.H.C. performed the mathematical modeling of mixture cell growth. A.S.L.W., G.C.G.C., C.H.C., and T.K.L. wrote the manuscript with help from all authors.

Fig. S1

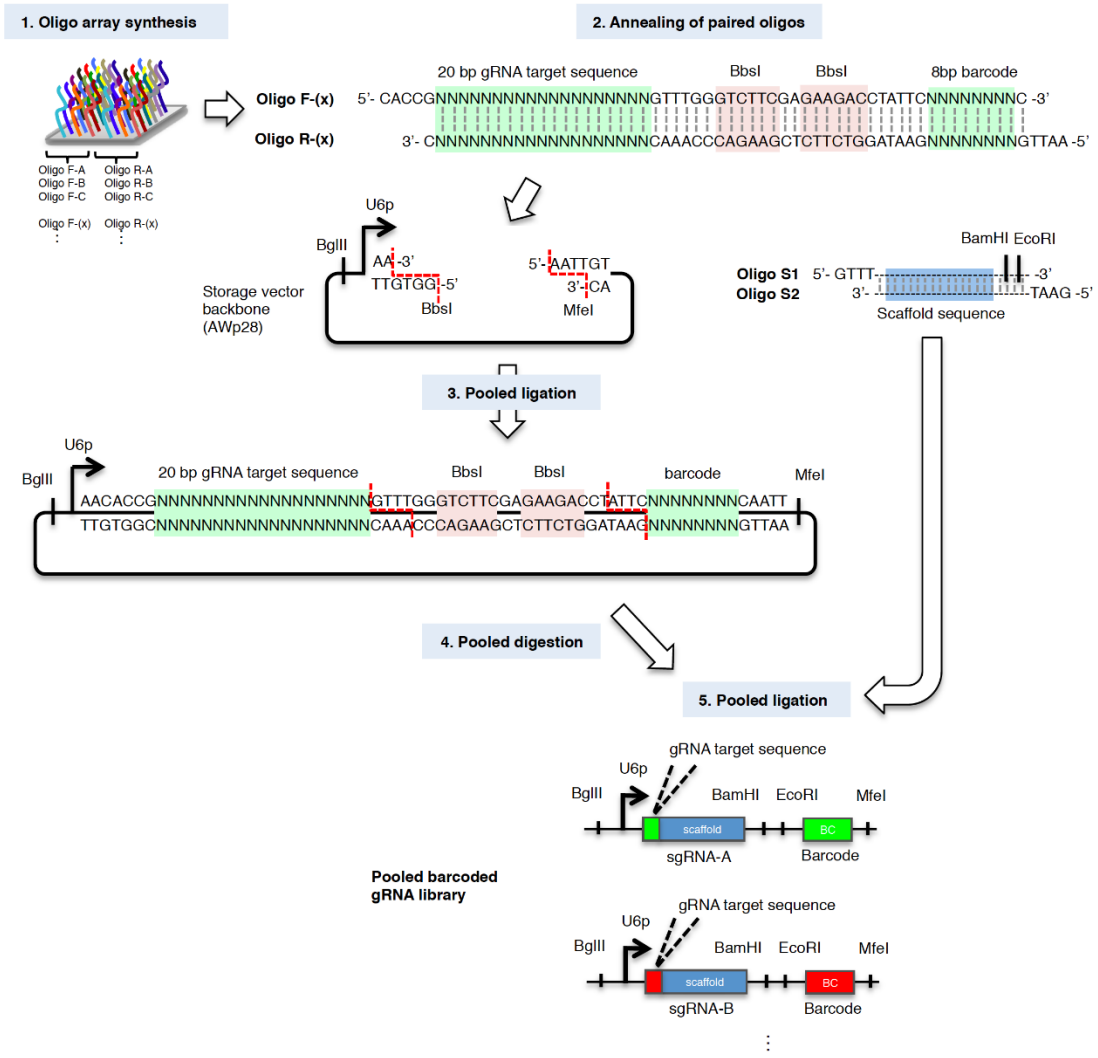

Fig. S1. Strategy for Assembling the Barcoded gRNA Library Pool. Forward and reverse oligo pairs (Oligo-F and Oligo-R, respectively) were synthesized and annealed to create double-stranded inserts with 20 bp gRNA target sequences, two BbsI sites, 8 bp barcodes, and 5' overhangs at their ends. To create the pooled storage vector library, the annealed inserts were mixed in 1:1 ratio and cloned in the storage vector (digested with BbsI and MfeI) with a one-pot ligation reaction via their compatible ends. To create the barcoded gRNA library pool, another single-pot ligation reaction was performed with the pooled storage vector library digested with BbsI, and an insert containing the gRNA scaffold sequence, BamHI and EcoRI sites, and 5' overhangs at their ends, which was generated via synthesis and annealing of Oligos S1 and S2.

Fig. S2

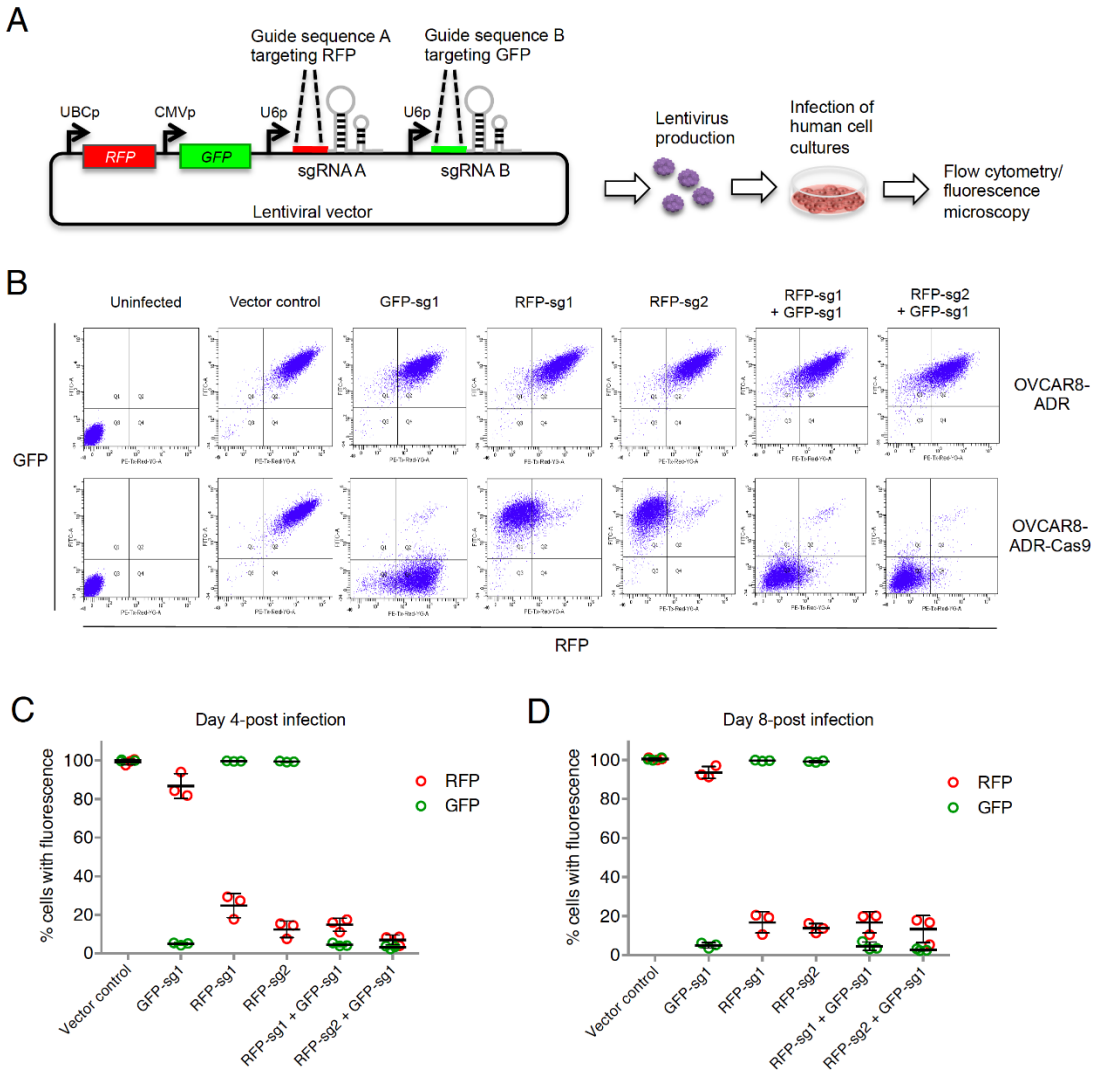
A
Guide sequence A targeting RFP
Guide sequence B targeting GFP
UBCp
CMVp
U6p
U6p
RFP
GFP
sgRNA A
sgRNA B
Lentiviral vector
Lentivirus production
Infection of human cell cultures
Flow cytometry/ fluorescence microscopy
B
Uninfected
Vector control
GFP-sg1
RFP-sg1
RFP-sg2
RFP-sg1 + GFP-sg1
RFP-sg2 + GFP-sg1
GFP
RFP
OVCAR8-ADR
OVCAR8-ADR-Cas9
C
Day 4-post infection
% cells with fluorescence
RFP
GFP
Vector control
GFP-sg1
RFP-sg1
RFP-sg2
RFP-sg1 + GFP-sg1
RFP-sg2 + GFP-sg1
D
Day 8-post infection
% cells with fluorescence
RFP
GFP
Vector control
GFP-sg1
RFP-sg1
RFP-sg2
RFP-sg1 + GFP-sg1
RFP-sg2 + GFP-sg1

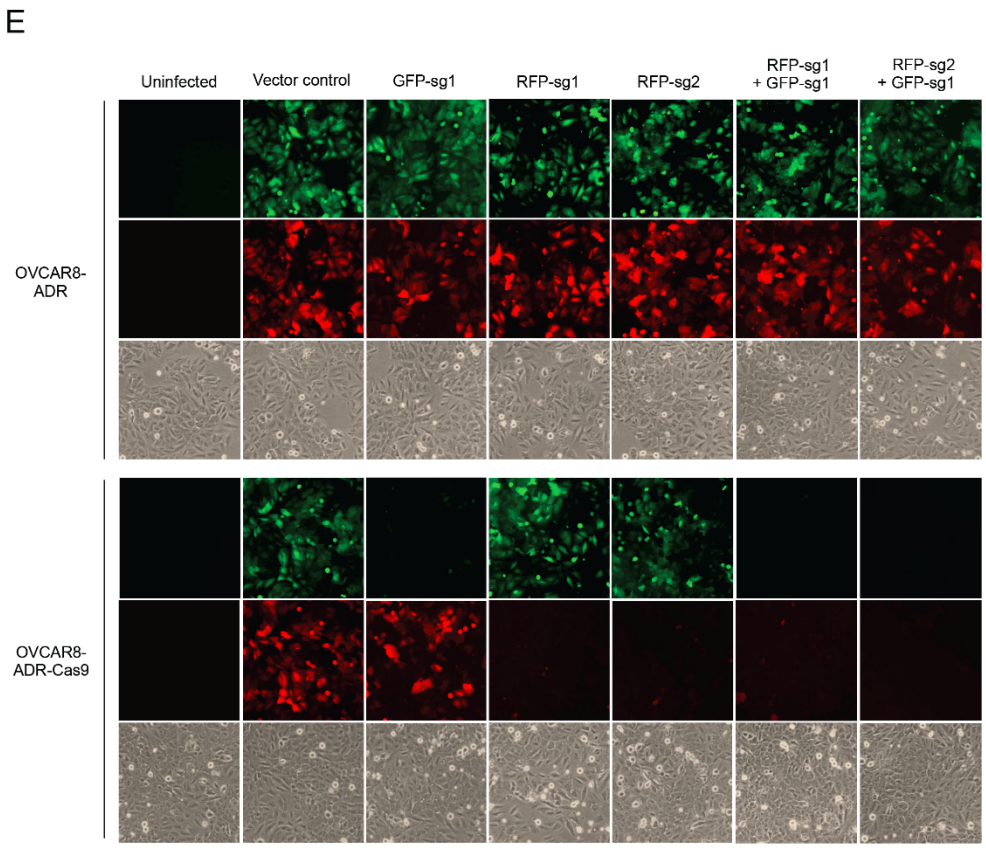

Fig. S2. Lentiviral Delivery of Combinatorial gRNA Expression Constructs Provides Efficient Target Gene Repression. (*A*) Strategy for testing lentiviral combinatorial gRNA expression constructs in human cells. We generated lentiviruses that contained *RFP* and *GFP* genes expressed from UBC and CMV promoters, respectively, and tandem U6 promoter-driven expression cassettes of gRNAs targeting *RFP* (RFP-sg1 or RFP-sg2) and *GFP* (GFP-sg1) sequences. These lentiviruses were delivered to OVCAR8-ADR or OVCAR8-ADR-Cas9 cells for analysis of GFP and RFP expression under flow cytometry and fluorescence microscopy. (*B* to *D*) Flow cytometry was used to measure cell populations positive for RFP and GFP fluorescence. Lentiviruses encoding combinatorial gRNA expression constructs reduced the percentage of cells positive for RFP and GFP fluorescence in OVCAR8-ADR-Cas9, but not OVCAR8-ADR, cells (*B*). The percentages of RFP- and GFP- positive cells were determined by flow cytometry at day 4 (*C*) and day 8 (*D*) post-infection. Limited cross-reactivity between sgRNAs targeting *RFP* and *GFP* were detected. Data in (*B*) represents flow cytometry measurements for cells infected for 4 days, while quantifications in both (*C*) and (*D*) represent

mean ± SD (n = 3). **(*E*)** Fluorescence microscopy revealed that combinatorial gRNA expression constructs effectively repressed RFP and GFP fluorescence levels in OVCAR8-ADR-Cas9, but not OVCAR8-ADR, cells at day 3 post-infection.

Fig. S3

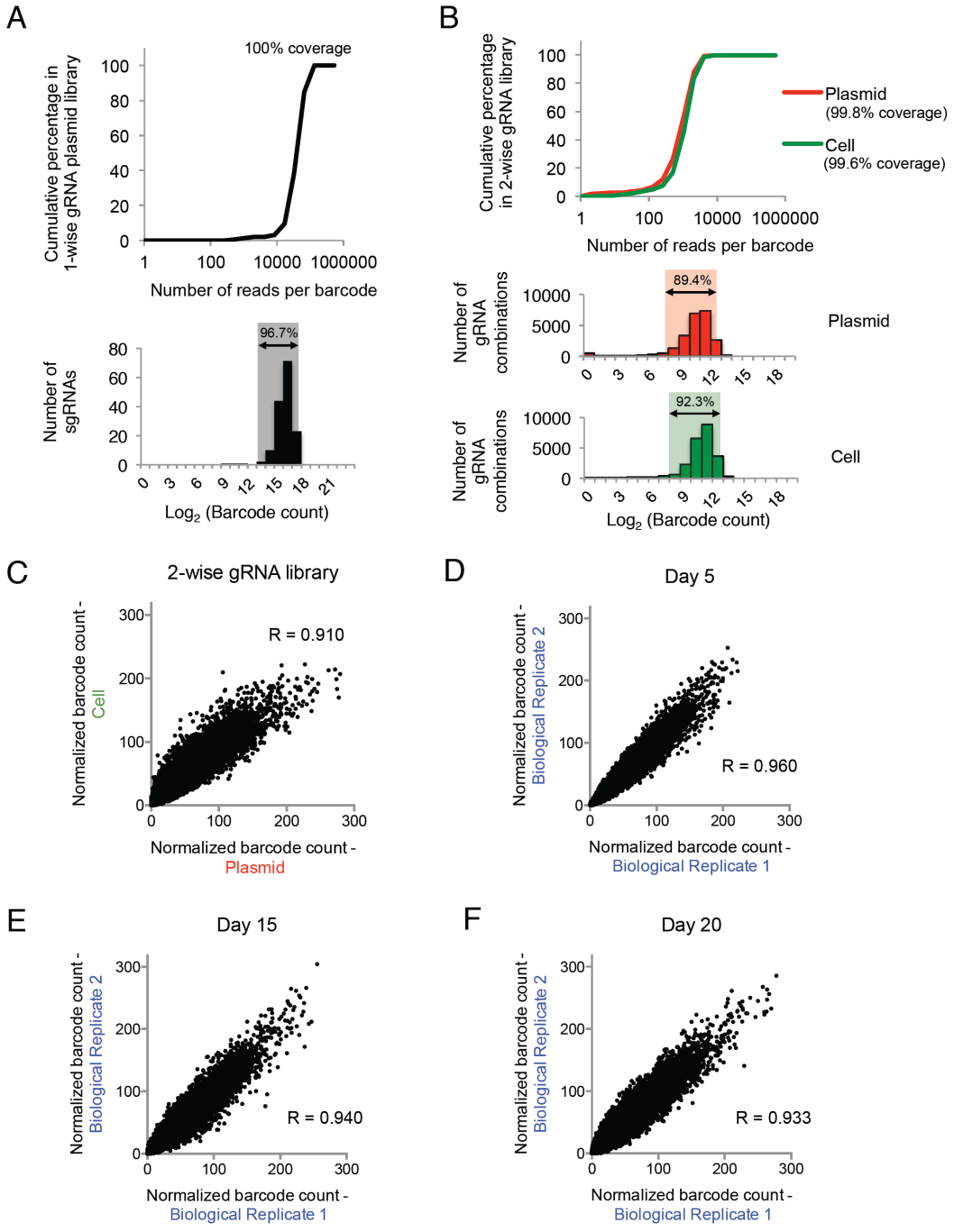

Fig. S3. Generation of a High-Coverage Combinatorial gRNA Library and Efficient Delivery of the Library to Human Cells. (*A* and *B*) Distributions of barcode reads for a one-wise gRNA library in the plasmid pool extracted from *E. coli* (*A*) and a two-wise gRNA library in both the plasmid pool and the lentivirus-infected OVCAR8-ADR-Cas9 cell pool (*B*) indicate high coverage for the expected combinations. Full coverage of all expected sgRNAs was

obtained in the plasmid pool (*A*), while 99.8% (i.e., 23,366 out of 23,409) and 99.6% (i.e., 23,324 out of 23,409) of the expected gRNA pairs were detected within the plasmid and infected cell pools, respectively (*B*). The missing gRNA pairs (i.e., with no barcode read) are listed in SI Appendix, Dataset S7. Most barcoded gRNA combinations were detected within a 5-fold range from the mean barcode reads per combination (highlighted by the shaded areas). (*C*) High correlations between barcode representations (normalized barcode counts) within the plasmid pool and infected OVCAR8-ADR-Cas9 cell pool indicate efficient lentiviral delivery of the two-wise library into human cells. (*D* to *F*) High reproducibility for barcode representations between two biological replicates in OVCAR8-ADR-Cas9 cells cultured for 5-day (*D*), 15-day (*E*) or 20-day (*F*) post-infection with the two-wise gRNA library. R is the Pearson correlation coefficient.

Fig. S4

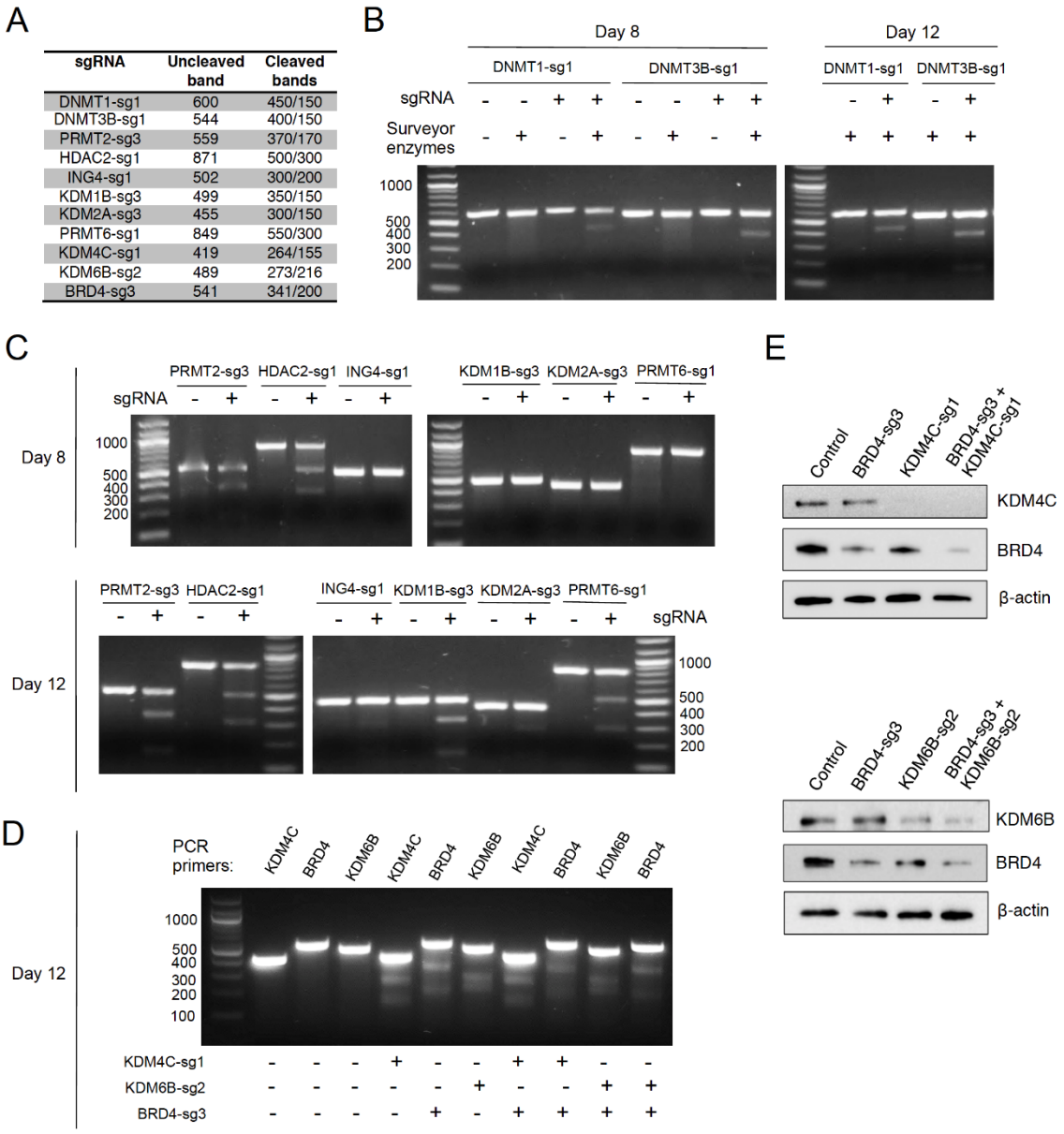

sgRNA	Uncleaved band	Cleaved bands
DNMT1-sg1	600	450/150
DNMT3B-sg1	544	400/150
PRMT2-sg3	559	370/170
HDAC2-sg1	871	500/300
ING4-sg1	502	300/200
KDM1B-sg3	499	350/150
KDM2A-sg3	455	300/150
PRMT6-sg1	849	550/300
KDM4C-sg1	419	264/155
KDM6B-sg2	489	273/216
BRD4-sg3	541	341/200

Fig. S4. Activity of gRNAs at Targeted Genomic Loci in OVCAR8-ADR-Cas9 Cells. (*A*) Summary table showing the expected sizes of the uncleaved and cleaved PCR products for the Surveyor assay. (*B* to *D*) Agarose gels showing the Surveyor assay results for DNA mismatch cleavage in OVCAR8-ADR-Cas9 cells that were either uninfected or infected with the indicated single- or dual- gRNA expression constructs selected from the screening library after 8 or 12 days post-infection. (*E*) Immunoblot analysis showing protein levels in OVCAR8-ADR-Cas9 cells that were either infected with vector control, or the indicated single- or dual- gRNA expression constructs for 15 days.

Fig. S5

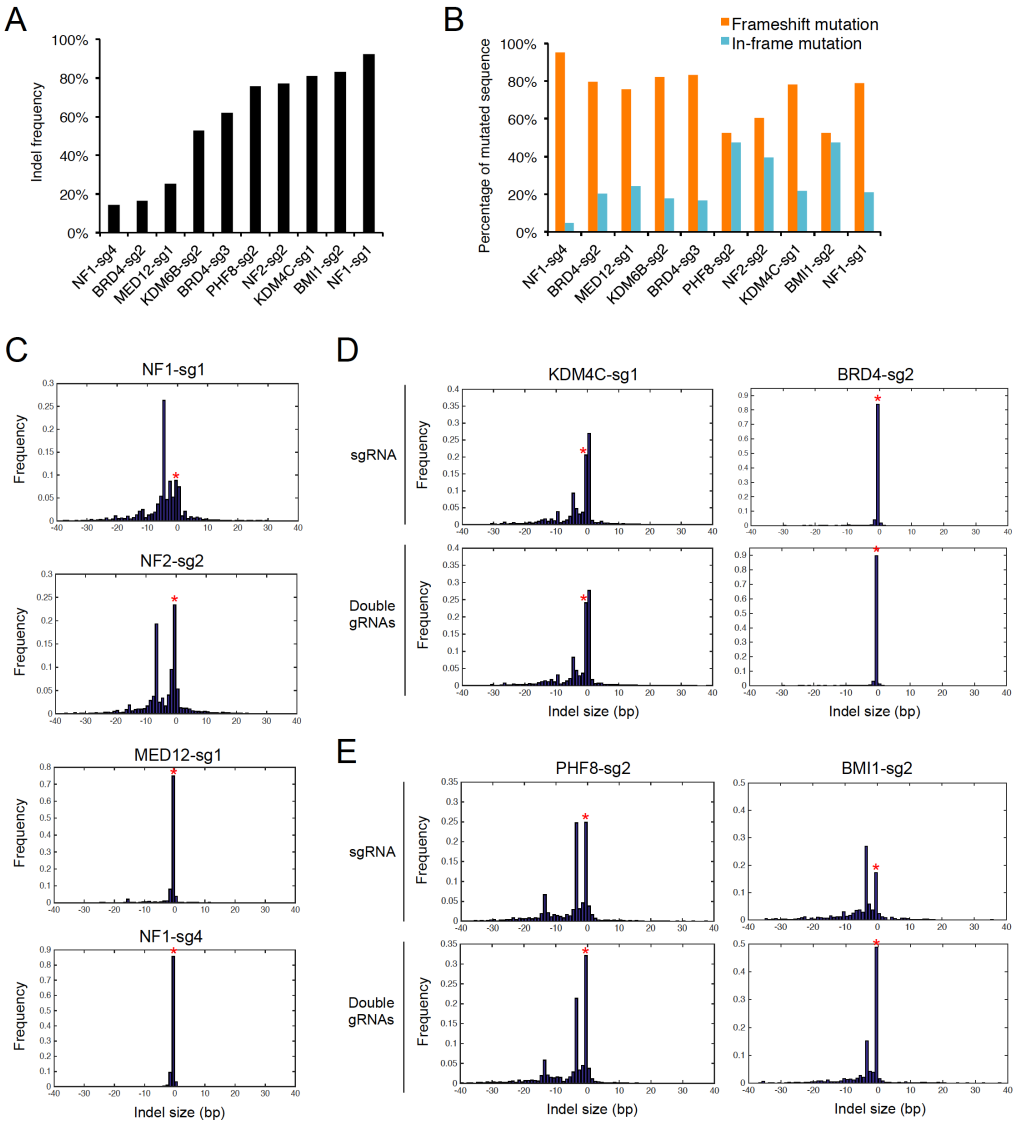

Fig. S5. Deep Sequencing for Indel Analysis at gRNA-Targeted Genomic Loci in OVCAR8-ADR-Cas9 cells. (*A* to *C*) Targeted genomic loci in OVCAR8-ADR-Cas9 cells infected with the indicated sgRNAs for 15 days were deep sequenced. The indel frequency (*A*), the percentage of frameshift and in-frame mutations (*B*), and the distribution of indel sizes (*C*) are shown. (*D* and *E*) The distribution of indels was analyzed by deep sequencing of the targeted genomic loci in OVCAR8-ADR-Cas9 cells that were either infected with the indicated sgRNA or dual-gRNA expression constructs for 15 days. In each sample, more than 4.2 million reads were used to analyze ~10,000 genomes extracted from the infected cells. The bar representing the wild-type sequence (i.e., with no indel) is labeled with a red asterisk in (*C*-*E*).

Fig. S6

A

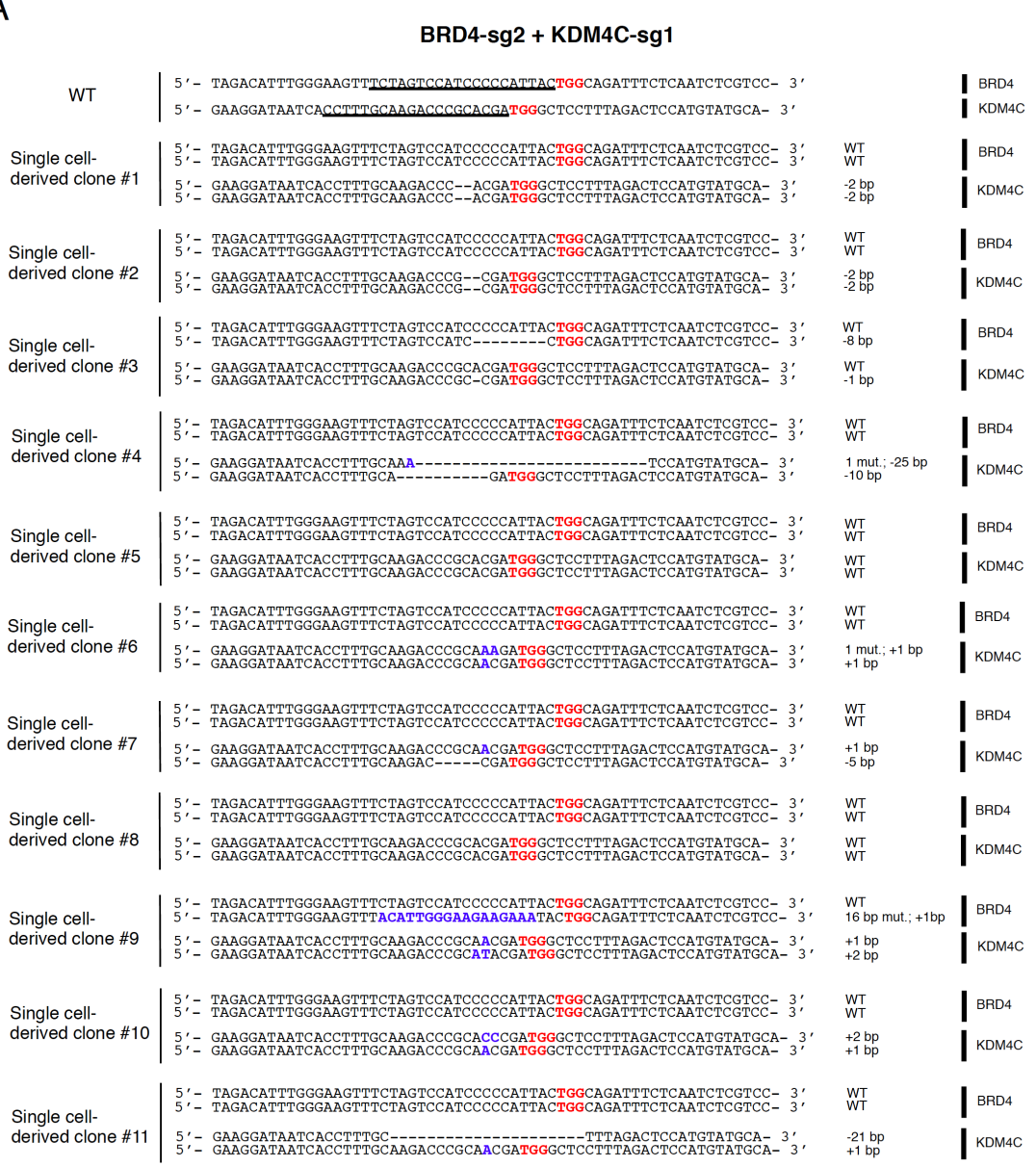
BRD4-sg2 + KDM4C-sg1
WT
5′- TAGACATTTGGGAAGTTTCTAGTCCATCCCCCATTACTGGCAGATTTCTCAATCTCGTCC- 3′
BRD4
5′- GAAGGATAATCACCTTTGCAAGACCCGCACGATGGGCTCCTTTAGACTCCATGTATGCA- 3′
KDM4C
Single cell-derived clone #1
5′- TAGACATTTGGGAAGTTTCTAGTCCATCCCCCATTACTGGCAGATTTCTCAATCTCGTCC- 3′ WT
5′- TAGACATTTGGGAAGTTTCTAGTCCATCCCCCATTACTGGCAGATTTCTCAATCTCGTCC- 3′ WT
BRD4
5′- GAAGGATAATCACCTTTGCAAGACCC--ACGATGGGCTCCTTTAGACTCCATGTATGCA- 3′ -2 bp
5′- GAAGGATAATCACCTTTGCAAGACCC--ACGATGGGCTCCTTTAGACTCCATGTATGCA- 3′ -2 bp
KDM4C
Single cell-derived clone #2
5′- TAGACATTTGGGAAGTTTCTAGTCCATCCCCCATTACTGGCAGATTTCTCAATCTCGTCC- 3′ WT
5′- TAGACATTTGGGAAGTTTCTAGTCCATCCCCCATTACTGGCAGATTTCTCAATCTCGTCC- 3′ WT
BRD4
5′- GAAGGATAATCACCTTTGCAAGACCCG--CGATGGGCTCCTTTAGACTCCATGTATGCA- 3′ -2 bp
5′- GAAGGATAATCACCTTTGCAAGACCCG--CGATGGGCTCCTTTAGACTCCATGTATGCA- 3′ -2 bp
KDM4C
Single cell-derived clone #3
5′- TAGACATTTGGGAAGTTTCTAGTCCATCCCCCATTACTGGCAGATTTCTCAATCTCGTCC- 3′ WT
5′- TAGACATTTGGGAAGTTTCTAGTCCATC---------CTGGCAGATTTCTCAATCTCGTCC- 3′ -8 bp
BRD4
5′- GAAGGATAATCACCTTTGCAAGACCCGCACGATGGGCTCCTTTAGACTCCATGTATGCA- 3′ WT
5′- GAAGGATAATCACCTTTGCAAGACCCGC-CGATGGGCTCCTTTAGACTCCATGTATGCA- 3′ -1 bp
KDM4C
Single cell-derived clone #4
5′- TAGACATTTGGGAAGTTTCTAGTCCATCCCCCATTACTGGCAGATTTCTCAATCTCGTCC- 3′ WT
5′- TAGACATTTGGGAAGTTTCTAGTCCATCCCCCATTACTGGCAGATTTCTCAATCTCGTCC- 3′ WT
BRD4
5′- GAAGGATAATCACCTTTGCAAA-------------------------TCCATGTATGCA- 3′ 1 mut.; -25 bp
5′- GAAGGATAATCACCTTTGCA-----------GATGGGCTCCTTTAGACTCCATGTATGCA- 3′ -10 bp
KDM4C
Single cell-derived clone #5
5′- TAGACATTTGGGAAGTTTCTAGTCCATCCCCCATTACTGGCAGATTTCTCAATCTCGTCC- 3′ WT
5′- TAGACATTTGGGAAGTTTCTAGTCCATCCCCCATTACTGGCAGATTTCTCAATCTCGTCC- 3′ WT
BRD4
5′- GAAGGATAATCACCTTTGCAAGACCCGCACGATGGGCTCCTTTAGACTCCATGTATGCA- 3′ WT
5′- GAAGGATAATCACCTTTGCAAGACCCGCACGATGGGCTCCTTTAGACTCCATGTATGCA- 3′ WT
KDM4C
Single cell-derived clone #6
5′- TAGACATTTGGGAAGTTTCTAGTCCATCCCCCATTACTGGCAGATTTCTCAATCTCGTCC- 3′ WT
5′- TAGACATTTGGGAAGTTTCTAGTCCATCCCCCATTACTGGCAGATTTCTCAATCTCGTCC- 3′ WT
BRD4
5′- GAAGGATAATCACCTTTGCAAGACCCGCAAAGATGGGCTCCTTTAGACTCCATGTATGCA- 3′ 1 mut.; +1 bp
5′- GAAGGATAATCACCTTTGCAAGACCCGCAACGATGGGCTCCTTTAGACTCCATGTATGCA- 3′ +1 bp
KDM4C
Single cell-derived clone #7
5′- TAGACATTTGGGAAGTTTCTAGTCCATCCCCCATTACTGGCAGATTTCTCAATCTCGTCC- 3′ WT
5′- TAGACATTTGGGAAGTTTCTAGTCCATCCCCCATTACTGGCAGATTTCTCAATCTCGTCC- 3′ WT
BRD4
5′- GAAGGATAATCACCTTTGCAAGACCCGCAACGATGGGCTCCTTTAGACTCCATGTATGCA- 3′ +1 bp
5′- GAAGGATAATCACCTTTGCAAGAC-----CGATGGGCTCCTTTAGACTCCATGTATGCA- 3′ -5 bp
KDM4C
Single cell-derived clone #8
5′- TAGACATTTGGGAAGTTTCTAGTCCATCCCCCATTACTGGCAGATTTCTCAATCTCGTCC- 3′ WT
5′- TAGACATTTGGGAAGTTTCTAGTCCATCCCCCATTACTGGCAGATTTCTCAATCTCGTCC- 3′ WT
BRD4
5′- GAAGGATAATCACCTTTGCAAGACCCGCACGATGGGCTCCTTTAGACTCCATGTATGCA- 3′ WT
5′- GAAGGATAATCACCTTTGCAAGACCCGCACGATGGGCTCCTTTAGACTCCATGTATGCA- 3′ WT
KDM4C
Single cell-derived clone #9
5′- TAGACATTTGGGAAGTTTCTAGTCCATCCCCCATTACTGGCAGATTTCTCAATCTCGTCC- 3′ WT
5′- TAGACATTTGGGAAGTTTACATTGGGAAGAAGAAATACTGGCAGATTTCTCAATCTCGTCC- 3′ 16 bp mut.; +1bp
BRD4
5′- GAAGGATAATCACCTTTGCAAGACCCGCAACGATGGGCTCCTTTAGACTCCATGTATGCA- 3′ +1 bp
5′- GAAGGATAATCACCTTTGCAAGACCCGCATACGATGGGCTCCTTTAGACTCCATGTATGCA- 3′ +2 bp
KDM4C
Single cell-derived clone #10
5′- TAGACATTTGGGAAGTTTCTAGTCCATCCCCCATTACTGGCAGATTTCTCAATCTCGTCC- 3′ WT
5′- TAGACATTTGGGAAGTTTCTAGTCCATCCCCCATTACTGGCAGATTTCTCAATCTCGTCC- 3′ WT
BRD4
5′- GAAGGATAATCACCTTTGCAAGACCCGCACCCGATGGGCTCCTTTAGACTCCATGTATGCA- 3′ +2 bp
5′- GAAGGATAATCACCTTTGCAAGACCCGCAACGATGGGCTCCTTTAGACTCCATGTATGCA- 3′ +1 bp
KDM4C
Single cell-derived clone #11
5′- TAGACATTTGGGAAGTTTCTAGTCCATCCCCCATTACTGGCAGATTTCTCAATCTCGTCC- 3′ WT
5′- TAGACATTTGGGAAGTTTCTAGTCCATCCCCCATTACTGGCAGATTTCTCAATCTCGTCC- 3′ WT
BRD4
5′- GAAGGATAATCACCTTTGC----------------------TTTAGACTCCATGTATGCA- 3′ -21 bp
5′- GAAGGATAATCACCTTTGCAAGACCCGCAACGATGGGCTCCTTTAGACTCCATGTATGCA- 3′ +1 bp
KDM4C

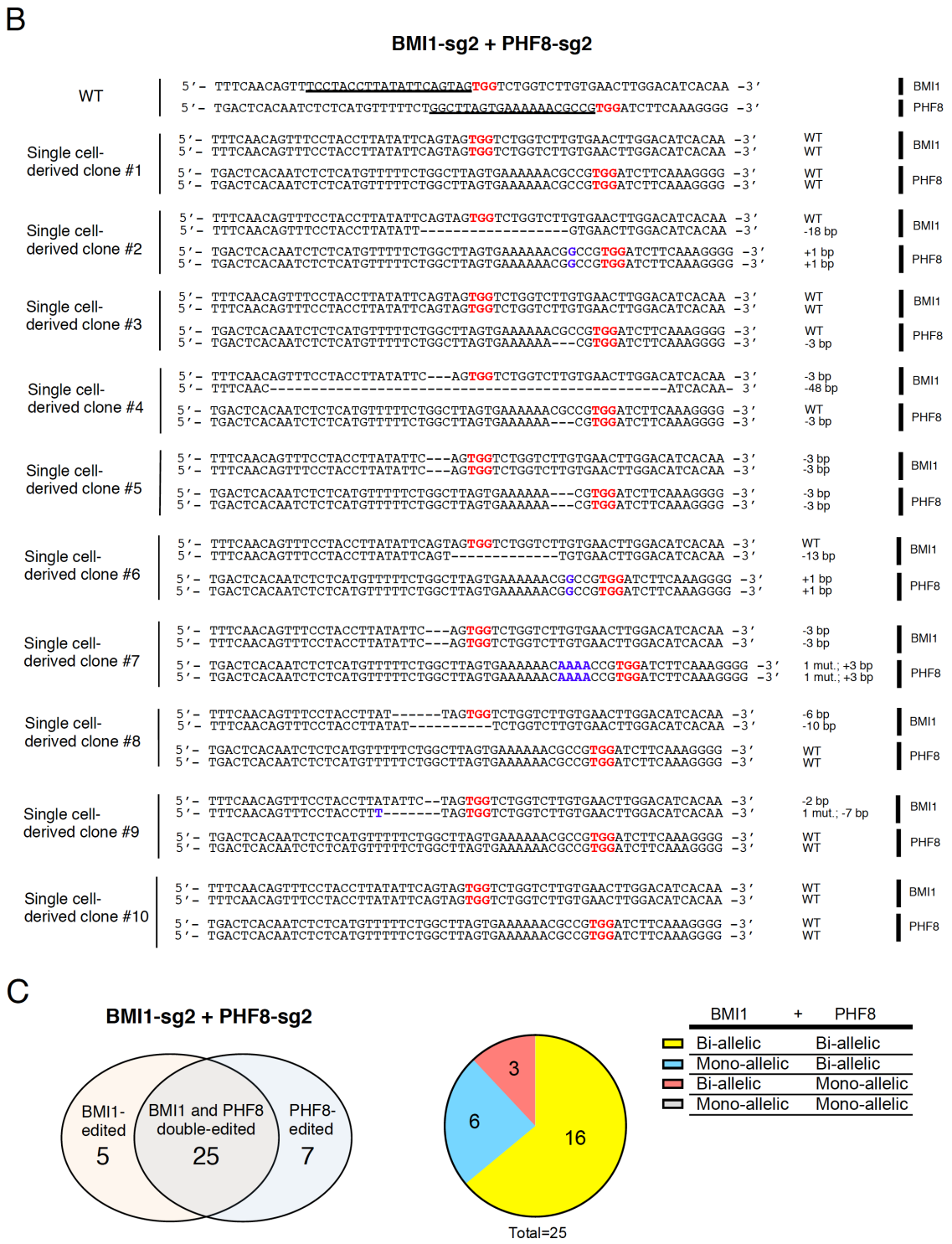

Fig. S6. Sequencing of Targeted Alleles for Individual OVCAR8-ADR-Cas9 Cells Infected with Dual-gRNA Expression Constructs. (*A* and *B*) OVCAR8-ADR-Cas9 cells infected with lentiviruses encoding the indicated dual-gRNA expression constructs for 12 days were plated as single cells. Genomic DNA for each single-cell-derived clone was extracted. The targeted alleles

were amplified by PCR and inserted into the TOPO vector by TA cloning for Sanger sequencing. The sequences for the two alleles of each clone are shown. Mutations and insertions are highlighted in blue, while deletions are indicated as "-". Wildtype (WT) sequences for the targeted genes are shown as references, with the 20 bp gRNA target and PAM sequences underlined and labeled in red, respectively. (*C*) Venn diagram showing the frequency of single- and dual- gene-edited cells (left panel). OVCAR8-ADR-Cas9 cells harboring the indicated dual-gRNA expression constructs were plated as single cells by FACS. The targeted alleles were sequenced from 40 whole genome-amplified single cells with Illumina MiSeq. 75% (i.e., 30/40) and 80% (i.e., 32/40) of the single cells harbored at least one mutant allele at the targeted BMI1 and PHF8 loci, respectively. 62.5% (i.e., 25/40) of the single cells contained at least one mutant allele in both BMI1 and PHF8 genes. Among the 25 cells that harbored both BMI1 and PHF8 mutant alleles, 16 of them were bi-allelic mutants for both genes while the other 9 cells harbored a mono-allelic mutation for one gene and bi-allelic mutations for the other gene (right panel). The sequences for the two alleles of each single cell are shown in SI Appendix, Dataset S3. We observed similar mutant allele frequencies determined from the single-cell-derived clones by Sanger sequencing (*B*) and whole-genome-amplified single cells by Illumina MiSeq (*C*).

Fig. S7

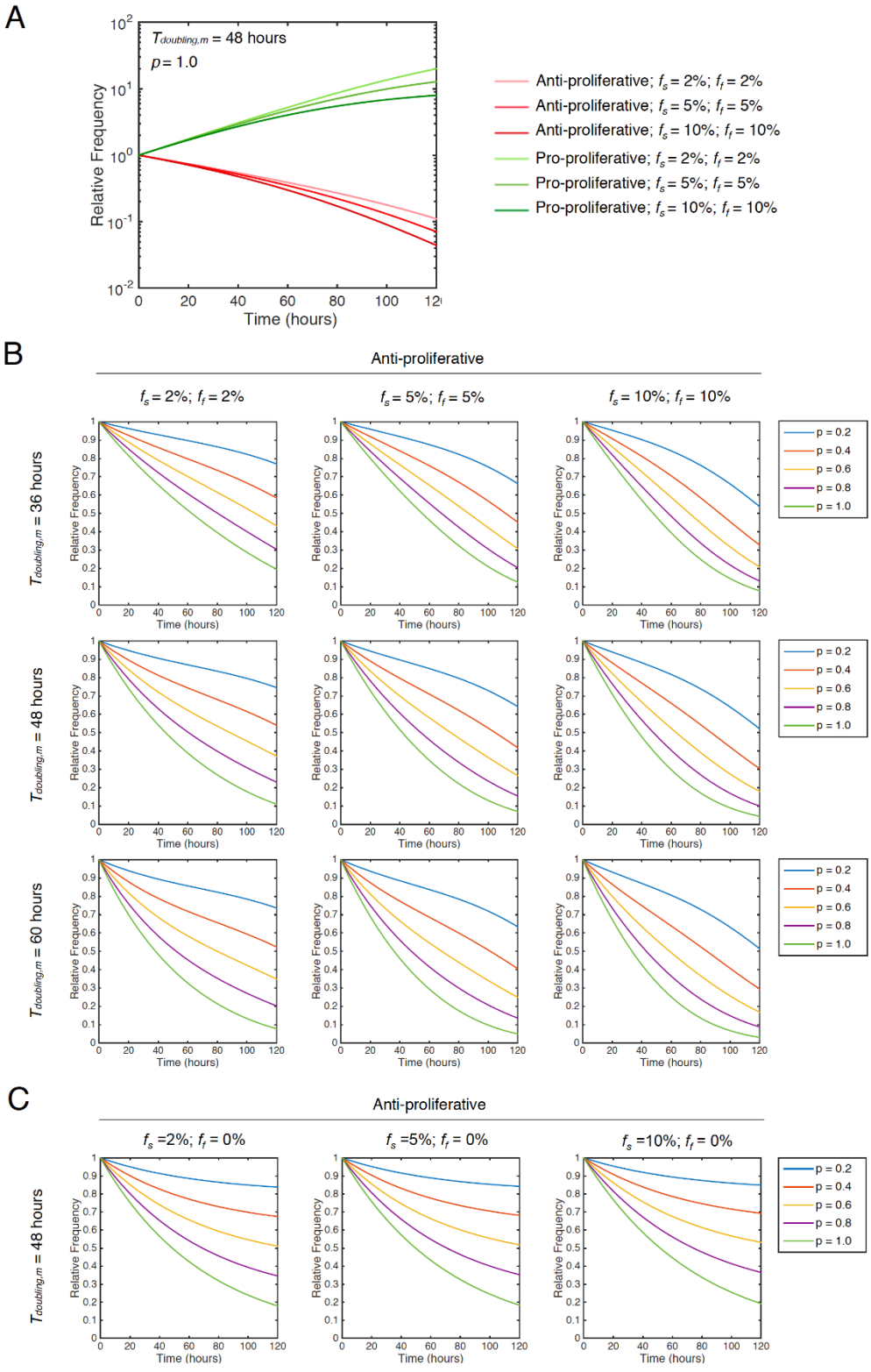
A
$T_{doubling,m}$ = 48 hours
p = 1.0
Relative Frequency
Time (hours)
Anti-proliferative; f_s = 2%; f_f = 2%
Anti-proliferative; f_s = 5%; f_f = 5%
Anti-proliferative; f_s = 10%; f_f = 10%
Pro-proliferative; f_s = 2%; f_f = 2%
Pro-proliferative; f_s = 5%; f_f = 5%
Pro-proliferative; f_s = 10%; f_f = 10%
B
Anti-proliferative
f_s = 2%; f_f = 2%
f_s = 5%; f_f = 5%
f_s = 10%; f_f = 10%
$T_{doubling,m}$ = 36 hours
$T_{doubling,m}$ = 48 hours
$T_{doubling,m}$ = 60 hours
p = 0.2
p = 0.4
p = 0.6
p = 0.8
p = 1.0
C
Anti-proliferative
f_s =2%; f_f = 0%
f_s =5%; f_f = 0%
f_s =10%; f_f = 0%
$T_{doubling,m}$ = 48 hours

Fig. S7. Mathematical Modeling of the Frequency of a Pro-Proliferative gRNA and an Anti-Proliferative gRNA within a Mixed Cell Population. (*A*) Simulation of the relative frequencies of a pro-proliferative gRNA (green) and an anti-proliferative (red) gRNA in a cell population with different fractions (i.e., 2, 5, or 10%) of cells that contain the anti-proliferative gRNA ($\boldsymbol{f_s}$) and the pro-proliferative ($\boldsymbol{f_f}$) gRNA initially. The relative frequency is defined as the barcode abundance at a given time compared to the initial time point. In this example, the fraction of cells with the modified growth rate due to genetic perturbations by the CRISPR-Cas9 system ($\boldsymbol{p}$) is set as 1.0 (i.e., 100%), and the doubling time of the anti-proliferative clone ($\boldsymbol{T_{doubling,m}}$) is 48 hours. (*B* and *C*) Modeled relative frequencies of an anti-proliferative gRNA in a mixed cell population with regard to variations in the parameters: $\boldsymbol{p}$, $\boldsymbol{T_{doubling,m}}$, $\boldsymbol{f_s}$, and $\boldsymbol{f_f}$. In (*A* to *C*), the doubling time of the pro-proliferative clone is set as 12 hours. Detailed definitions are described in SI Appendix, SI Materials and Methods.

Fig. S8

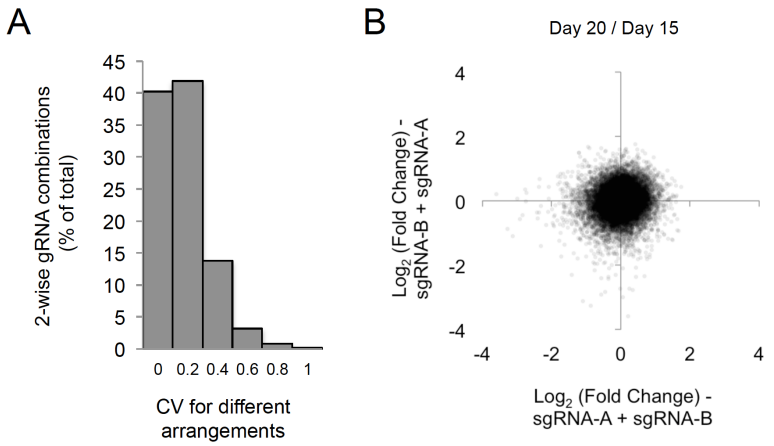

Fig. S8. Fold-Changes in Barcodes among the Same gRNA Combinations Arranged in Different Orders in the Expression Constructs. (*A*) The coefficient of variation (CV; defined as SD/mean of the fold changes of normalized barcode counts for 20-day versus 15-day cultured OVCAR8-ADR-Cas9 cells) was determined for the same two-wise gRNA combination arranged in the two possible different orders (i.e., *sgRNA-A* + *sgRNA-B* and *sgRNA-B* + *sgRNA-A*) among two biological replicates. Over 82% and 95% of two-wise gRNA combinations had a CV of <0.2 and <0.4, respectively, in the cell-proliferation screen. (*B*) Scatter plot showing the $\log_2$ ratios of the normalized barcode counts for 20-day versus 15-day cultured cells between the same two-wise gRNA combinations arranged in the two possible different orders.

Fig. S9

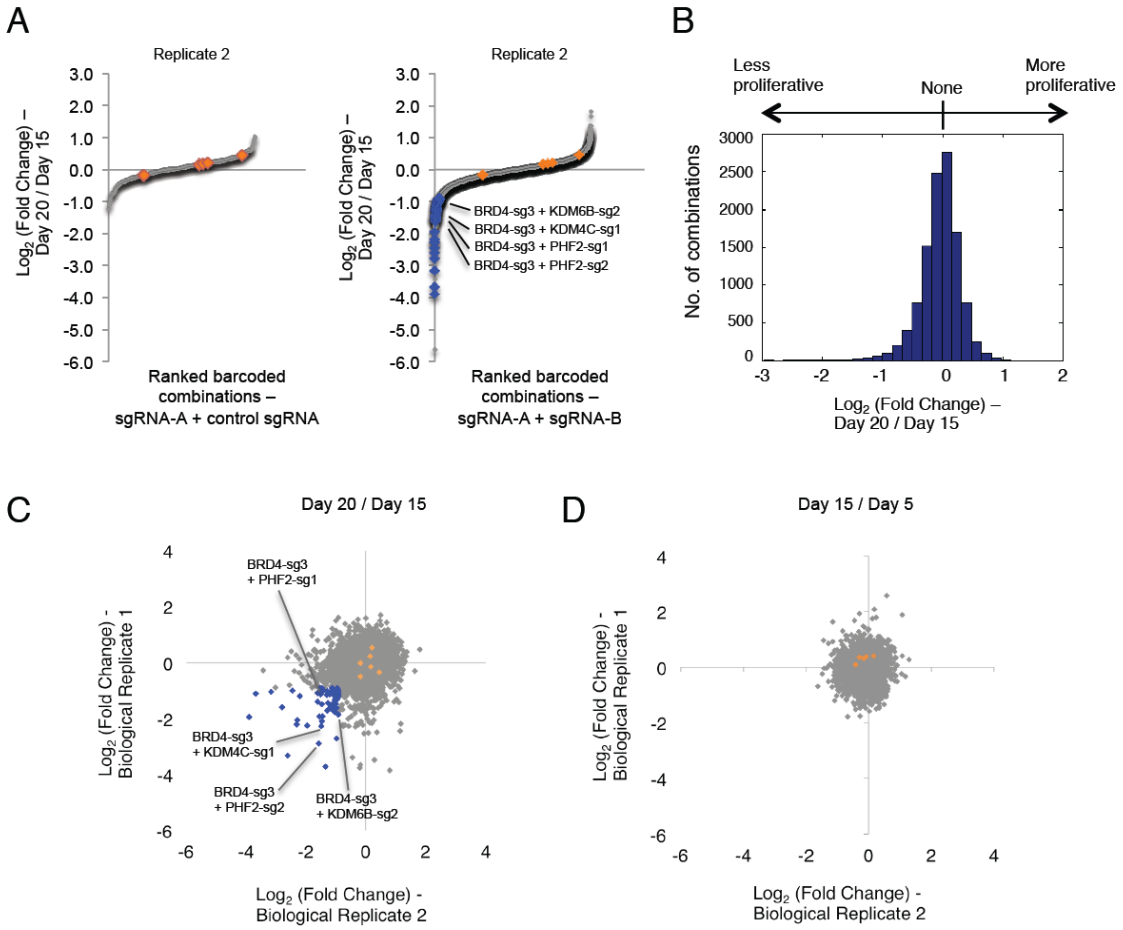

Fig. S9. Biological Replicates and Log_2 Fold-Change Comparisons for the Combinatorial Screen Used to Identify gRNA Pairs that Inhibit Cancer Cell Proliferation. (*A*) OVCAR8-ADR-Cas9 cells were infected with the same two-wise gRNA library used in Fig. 3*B*. Guide RNA pairs (right panel) and their sgRNA + control counterparts (i.e., gene-targeting sgRNA + control sgRNA; left panel) that modulated proliferation were ranked by their log_2 ratios of the normalized barcode count for 20-day versus 15-day cultured cells. The anti-proliferative effects of gRNA combinations that were confirmed in another biological replicate (Fig. 2*B*) are highlighted in blue, while combinations with control gRNA pairs are highlighted in orange. Same colors are used in panels (*C*) and (*D*). Labeled gRNA combinations were further validated in this study (Fig. 2*C*). (*B*) Frequency distribution of log_2 ratios for the gRNA combinations in the pooled screen. Log_2 ratios shown were calculated from the mean of two biological replicates. (*C* and *D*) Scatter plots showing the log_2 ratios of the normalized barcode counts for 20-day

versus 15-day (*C*) and 15-day versus 5-day (*D*) cultured cells between two biological replicates of OVCAR8-ADR-Cas9 cells infected with the two-wise gRNA library. Only relatively minor changes in the representation of combinations were observed between day 5 and day 15.

Fig. S10

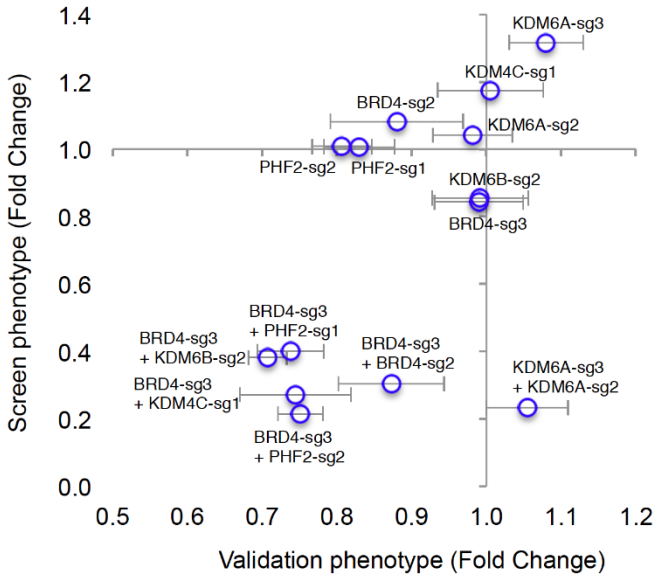

Fig. S10. Pooled Screen and Validation Data for Individual gRNA Combinations. For each gRNA combination, the fold-change in the normalized barcode count for 20-day versus 15-day cultured cells obtained from the pooled screening data ('Screen phenotype') was plotted against its relative cell viability compared to the vector control determined from the individual cell-proliferation assays ('Validation phenotype'). The 'Screen phenotype' of each individual sgRNA was averaged from the fold-change of the corresponding sgRNA paired with each of the three control sgRNAs. Data for the screening data are the mean of two biological replicates, while the individual validation data represent the mean ± SD ($n \geq 3$).

Fig. S11

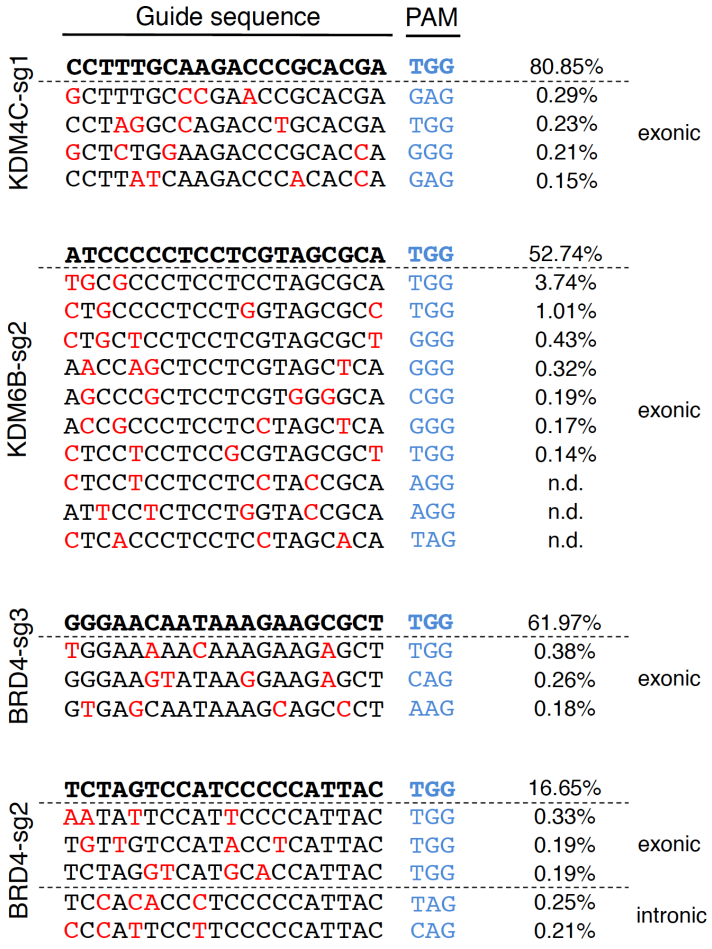

Fig. S11. Measurement of On-Target and Off-Target Indel Generation Rates for gRNAs Targeting KDM4C, KDM6B and BRD4. Each row represents a genomic locus corresponding to a 20 bp guide sequence (in black letters) followed by a 3 bp PAM sequence (in blue letters). Sequences in bold black letters represent the gRNA's on-target genomic sequence. Below each bold line for KDM4C-sg1, KDM6B-sg2, and BRD4-sg3 are the predicted exonic off-target genomic sequences identified using the CRISPR design(8) and CCTop(9) tools. Five exonic/intronic off-target sites predicted for BRD4-sg2 were also evaluated. Red nucleotides highlight the differences in the off-target sequences from the on-target sequence. Each genomic locus was PCR amplified from ~10,000 cells and deep sequenced with >4.2 million reads. n.d. indicates that PCR of the genomic sequence failed to provide specific amplicons for sequencing.

Fig. S12

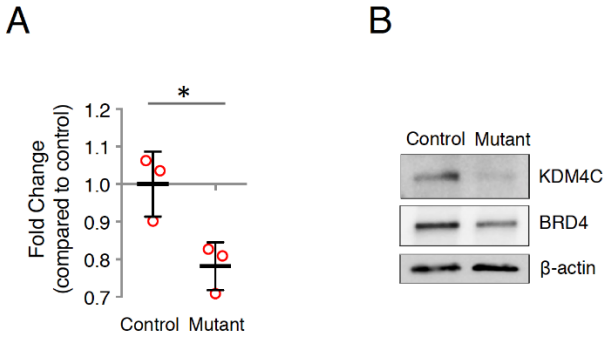

Fig. S12. Reduced Growth in OVCAR8-ADR-Cas9 Cells Harboring Both KDM4C and BRD4 Frameshift Mutations. (*A*) Cell growth assay on a single-cell-expanded OVCAR8-ADR-Cas9 mutant clone with both *KDM4C* and *BRD4* frameshift mutations (i.e., derived from Clone #3 shown in SI Appendix, Fig. S6*A*). Equal numbers of cells were plated and cultured for 5 days before MTT assay. Data represent mean ± SD (n = 3) of absorbance measurements (OD_{570} - OD_{650}) relative to control OVCAR8-ADR-Cas9 cells. The asterisk (*P < 0.01) represents significant difference between the control and mutant cells. (*B*) Immunoblot analysis of protein levels in the control and mutant cells from (*A*).

Fig. S13

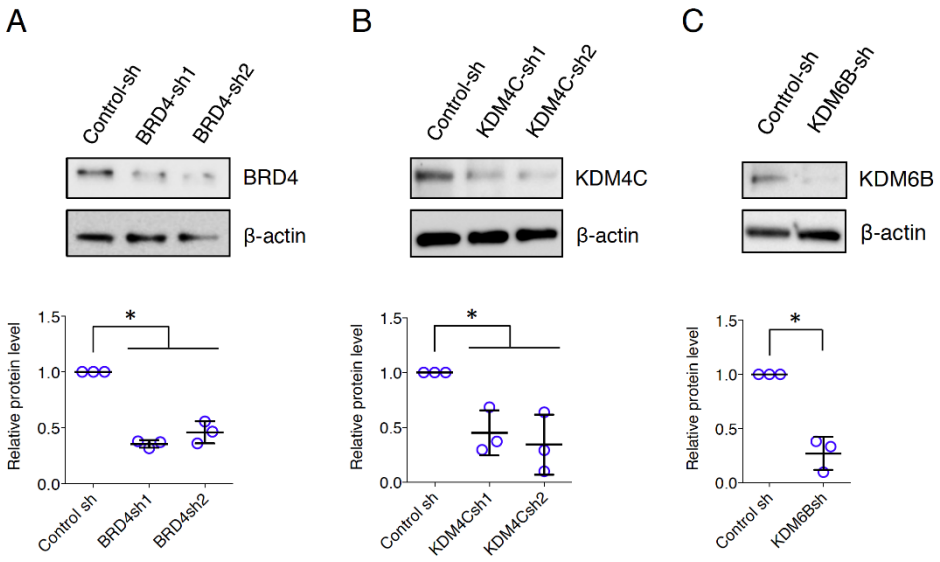

Fig. S13. shRNA-Mediated Knockdown of Targeted Genes in OVCAR8-ADR Cells. (*A* to *C*) Immunoblot analysis of relative protein levels in OVCAR8-ADR cells expressing control shRNA or shRNAs targeting *KDM4C*, *BRD4*, or *KDM6B*. Measured protein levels were normalized to actin levels, and then were normalized to the control shRNA samples. Data represent mean ± SD (n = 3). The asterisk (*P < 0.05) represents a significant difference in protein levels between cells expressing the gene-targeting shRNA versus control shRNA.

Fig. S14

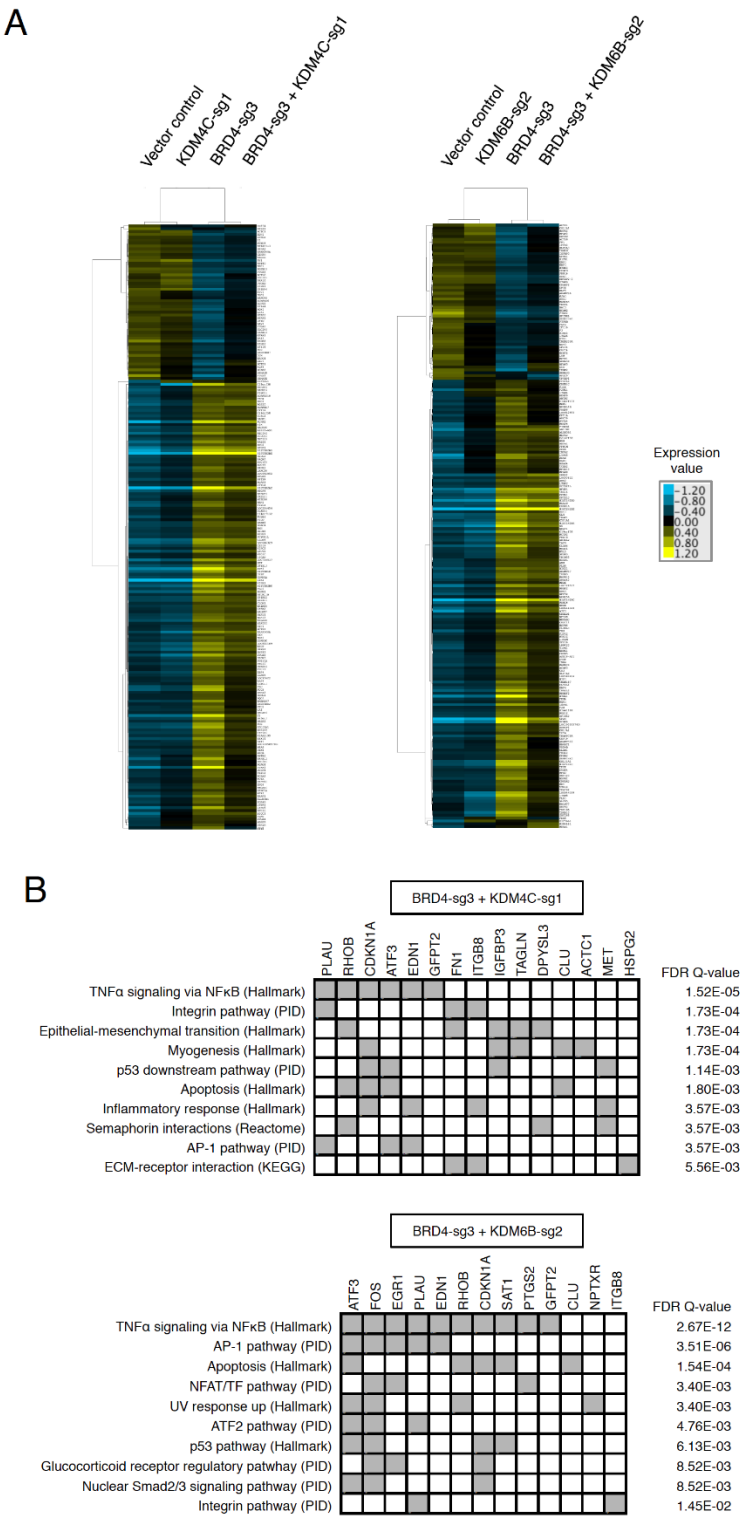
A
Vector control
KDM4C-sg1
BRD4-sg3
BRD4-sg3 + KDM4C-sg1
Vector control
KDM6B-sg2
BRD4-sg3
BRD4-sg3 + KDM6B-sg2
Expression value
1.20
0.80
0.40
0.00
0.40
0.80
1.20
B
BRD4-sg3 + KDM4C-sg1
PLAU
RHOB
CDKN1A
ATF3
EDN1
GFPT2
FN1
ITGB8
IGFBP3
TAGLN
DPYSL3
CLU
ACTC1
MET
HSPG2
FDR Q-value
TNFα signaling via NFκB (Hallmark) 1.52E-05
Integrin pathway (PID) 1.73E-04
Epithelial-mesenchymal transition (Hallmark) 1.73E-04
Myogenesis (Hallmark) 1.73E-04
p53 downstream pathway (PID) 1.14E-03
Apoptosis (Hallmark) 1.80E-03
Inflammatory response (Hallmark) 3.57E-03
Semaphorin interactions (Reactome) 3.57E-03
AP-1 pathway (PID) 3.57E-03
ECM-receptor interaction (KEGG) 5.56E-03
BRD4-sg3 + KDM6B-sg2
ATF3
FOS
EGR1
PLAU
EDN1
RHOB
CDKN1A
SAT1
PTGS2
GFPT2
CLU
NPTXR
ITGB8
FDR Q-value
TNFα signaling via NFκB (Hallmark) 2.67E-12
AP-1 pathway (PID) 3.51E-06
Apoptosis (Hallmark) 1.54E-04
NFAT/TF pathway (PID) 3.40E-03
UV response up (Hallmark) 3.40E-03
ATF2 pathway (PID) 4.76E-03
p53 pathway (Hallmark) 6.13E-03
Glucocorticoid receptor regulatory patwhay (PID) 8.52E-03
Nuclear Smad2/3 signaling pathway (PID) 8.52E-03
Integrin pathway (PID) 1.45E-02

Fig. S14. RNA-Sequencing Analysis of OVCAR8-ADR-Cas9 Cells Infected with gRNA Expression Constructs. (*A*) Heatmaps showing the relative expression levels of each gene transcript (rows) in each sample (column), which were OVCAR8-ADR-Cas9 cells targeted by the respective single or dual gRNAs. Transcripts that were identified as significantly differentially expressed in OVCAR8-ADR-Cas9 cells infected with the indicated gRNA(s), when compared to the vector control, are included in the heatmaps. Expression values are $\log_2$-transformed FPKM measured using RNA-Seq, and mean-centered by the transcript. Hierarchical clustering of transcripts and samples was performed based on the Pearson's correlation. (*B*) Top ten enriched gene sets of biological processes for the differentially expressed genes identified in OVCAR8-ADR-Cas9 cells infected with the indicated gRNAs when compared to the vector control (Q-value <0.05). Subsets of the differentially expressed genes (x-axes) that are associated with the gene sets (y-axes) are shaded in grey in the tables.

Fig. S15

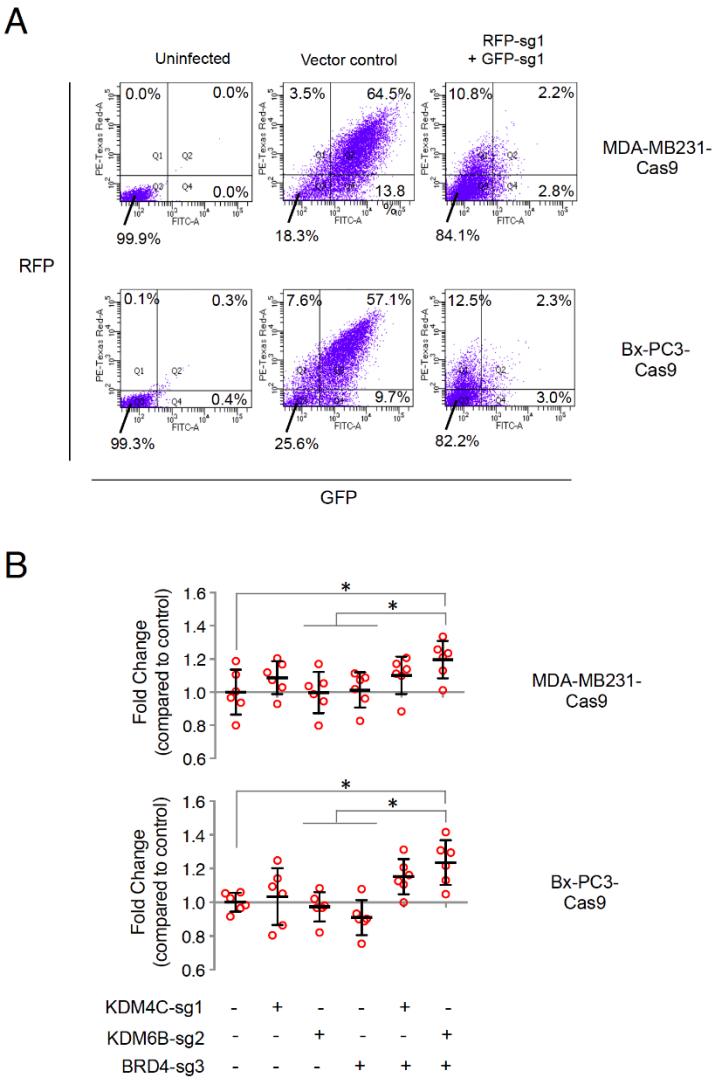

Fig. S15. Effect of KDM4C and BRD4, as well as KDM6B and BRD4, on Cell Growth for Additional Cancer Cell Lines. (*A*) Combinatorial gRNA expression constructs effectively repressed targeted fluorescence genes in breast cancer MDA-MB231-Cas9 and pancreatic cancer Bx-PC3-Cas9 cells. Lentiviral vectors that contained RFP and GFP genes expressed from constitutive promoters, with or without tandem U6 promoter-driven expression cassettes of gRNAs targeting RFP and GFP sequences, were delivered to MDA-MB231-Cas9 and Bx-PC3-Cas9 cells for analysis of GFP and RFP expression under flow cytometry. Detailed strategy is described in SI Appendix, Fig. S2. Lentiviruses encoding combinatorial gRNA expression constructs reduced the percentage of cells positive for RFP and GFP fluorescence at day 4 post-

infection. (*B*) MDA-MB231-Cas9 and Bx-PC3-Cas9 cells infected with lentiviruses expressing the indicated single or combinatorial gRNAs were cultured for 14 days. Equal numbers of infected cells were then re-plated and cultured for additional 5 days. Cell viabilities relative to control sgRNA were determined by the MTT assay. Data represent mean ± SD (n =6) from biological replicates. The asterisk (*$P < 0.05$) represents significant differences between the indicated samples. These results indicate that combinatorial gRNA targeting of genes can have variable phenotypes depending on the cellular background.

Dataset S1. sgRNA Target Sequences Used in this Study

sgRNA ID	sgRNA target sequence
GFP-sg1	GGGCGAGGAGCTGTTCACCG
RFP-sg1	CACCCAGACCATGAAGATCA
RFP-sg2	CCACTTCAAGTGCACATCCG
NF1-sg1	GTTGTGCTCAGTACTGACTT
NF1-sg4	TTTCAGCTTCCAATAAAAAC
NF2-sg2	ATTCCACGGGAAGGAGATCT
MED12-sg1	AGGATTGAAGCTGACGTTCT
Control-sg1	ATCGTTTCCGCTTAACGGCG
Control-sg2	AAACGGTACGACAGCGTGTG
Control-sg3	CCATCACCGATCGTGAGCCT
DNMT1-sg1	CTAGACGTCCATTCACTTCC
DNMT1-sg2	TTTCCAAACCTCGCACGCCC
DNMT1-sg3	ACGTAAAGAAGAATTATCCG
DNMT3A-sg1	CCGCCCCACCTTCCGTGCCG
DNMT3A-sg2	TGGCGCTCCTCCTTGCCACG
DNMT3A-sg3	CCGCTCCGCAGCAGAGCTGC
DNMT3B-sg1	AGAGTCGCGAGCTTGATCTT
DNMT3B-sg2	ATCCGCACCCCGGAGATCAG
DNMT3B-sg3	GAAGACTCGATCCTCGTCAA
DNMT3L-sg1	AGGGATCTGCGCCCCATGTA
DNMT3L-sg2	ACTCACCTTCTATATTTCGC
DNMT3L-sg3	CACCAAAATCACGTCCATGC
MBD1-sg1	TCACCCGTAGGCAACGTCGC
MBD1-sg2	GTGTCCAGCGACGTTGCCTA
MBD1-sg3	ACGTTGTGCAAAGACTGTCG
MBD2-sg1	CGGCGACTCCGCCATAGAGC
MBD2-sg2	GGAGCCGGTCCCTTTCCCGT
MBD2-sg3	AGTCTTGAAAGCGCATGCCA
CREBBP-sg1	AGCGGCTCTAGTATCAACCC
CREBBP-sg2	GAATCACATGACGCATTGTC
CREBBP-sg3	CCCGCAAATGACTGGTCACG
EP300-sg1	CTGTCAGAATTGCTGCGATC
EP300-sg2	CTTGGCAAGACTTGCCTGAC
EP300-sg3	TAGTTCCCCTAACCTCAATA
HDAC1-sg1	ACACCATTCGTAACGTTGCC
HDAC1-sg2	TCACTCGAGATGCGCTTGTC
HDAC1-sg3	AGAATGCTGCCGCACGCACC
HDAC2-sg1	TCCGTAATGTTGCTCGATGT
HDAC2-sg2	TCCAACATCGAGCAACATTA

HDAC2-sg3	TACAACAGATCGTGTAATGA
SIRT1-sg1	GTTGACTGTGAAGCTGTACG
SIRT1-sg2	AACAGGTTGCGGGAATCCAA
SIRT1-sg3	TACCCAGAACATAGACACGC
CARM1-sg1	CTCGCCGTTCGCGTCGCCGA
CARM1-sg2	CCCGTACTCACGGCTGTAGA
CARM1-sg3	GGGCCACGTACCGTTGGGTG
EZH1-sg1	ACAGGCTTCATTGACTGAAC
EZH1-sg2	AGCTGATCAATAACTATGAT
EZH1-sg3	CCTCATCTGAGTACTGATTC
EZH2-sg1	ACACGCTTCCGCCAACAAAC
EZH2-sg2	TGCGACTGAGACAGCTCAAG
EZH2-sg3	AAAACTTCATCTCCCATATA
MLL-sg1	GTACAAATTGTACGACGGAG
MLL-sg2	GACCCCTCGGCGGTTTATAG
MLL-sg3	TATATTGCGACCACCAAACT
MLL2-sg1	CAGAGAGCACAACGCCGCAC
MLL2-sg2	GGAACCGCTGGCAGTCGCGC
MLL2-sg3	CTCCCGCTGCCCGTGTAGAC
NSD1-sg1	CTGGCTCGAGATTTAGCGCA
NSD1-sg2	AATCTGTTCATGCGCTTACG
NSD1-sg3	GATTCCAGTACCAGTACATT
PRMT1-sg1	CTCACCGTGGTCTAACTTGT
PRMT1-sg2	GGATGTCATGTCCTCAGCGT
PRMT1-sg3	TTTGACTCCTACGCACACTT
PRMT2-sg1	CGTGGATGAGTACGACCCCG
PRMT2-sg2	TCTTCTGTGCACACTATGCG
PRMT2-sg3	CTGTCCCAGAAGTGAATCGC
PRMT3-sg1	GCCATGTGCTCGTTAGCGTC
PRMT3-sg2	GCCTGACGCTAACGAGCACA
PRMT3-sg3	GAATTCATGTACTCAACTGT
PRMT5-sg1	CGGAATGCGGGGTCCGAACT
PRMT5-sg2	CAGCATACAGCTTTATCCGC
PRMT5-sg3	ATGAACTCCCTCTTGAAACG
PRMT6-sg1	ATTGTCCGGCGAGGACGTGC
PRMT6-sg2	CTTCGCCACGCGCTGTCTCA
PRMT6-sg3	GACGGTACTGGACGTGGGCG
PRMT7-sg1	CAATCCGACCACGGGGTCTG
PRMT7-sg2	GAGGTTCAAACCGCCTGCTA
PRMT7-sg3	TAAAGTCGGCTGGTGACACC
SETD2-sg1	AGTTCTTCTCGGTGTCCAAA

SETD2-sg2	GACTATCAGTTCCAGAGATA
SETD2-sg3	AACTTACGAAGGAAGGTCTT
KDM1A-sg1	TTACCTTCGCCCGCTTGCGC
KDM1A-sg2	CCGGCCCTACTGTCGTGCCT
KDM1A-sg3	AGAGCCGACTTCCTCATGAC
KDM1B-sg1	CATACCGCATCGATAAGTCT
KDM1B-sg2	ATAGCCAAGACTTATCGATG
KDM1B-sg3	GAACATACCTTCTGTAGTAA
KDM2A-sg1	ACGCTACTATGAGACCCCAG
KDM2A-sg2	TATGGCAGGGAGTCGTCGCA
KDM2A-sg3	GTAACGAATCCTTTCTTCTT
KDM2B-sg1	CCTCGTTCTCGTCGTATCGC
KDM2B-sg2	GCGTTACTACGAGACGCCCG
KDM2B-sg3	CTTGGTCAAGCGTCCGACTG
KDM3A-sg1	TAAATGCCGAGAGTGTCGCT
KDM3A-sg2	GTCTGTCAAAACCGACTTCC
KDM3A-sg3	GATACTGCTTGGCTGTACTG
KDM3B-sg1	TCTTGTATGGGCGCCCCGTG
KDM3B-sg2	GCCTTGACTGTTACCGGCTC
KDM3B-sg3	TCCTGAGCCGGTAACAGTCA
KDM4A-sg1	ACTCCGCACAGTTAAAACCA
KDM4A-sg2	GCGGAACTCTCGAACAGTCA
KDM4A-sg3	TTCCACTCACTTATCGCTAT
KDM4B-sg1	CCCCGCGTACTTCTCGCTGT
KDM4B-sg2	GTATGATGACATCGACGACG
KDM4B-sg3	TCACCAGGTACTGTACCCCG
KDM4C-sg1	CCTTTGCAAGACCCGCACGA
KDM4C-sg2	AGTAGGCTTCGTGTGATCAA
KDM4C-sg3	GTCTAAAGGAGCCCATCGTG
KDM5A-sg1	CATGAACCCCAACGTGCTAA
KDM5A-sg2	CTGGGATTCAAATAACTCGG
KDM5A-sg3	TCTCTGGTATGAAAGTGCCG
KDM5B-sg1	GTCCGCGAACTCTTCCCAGC
KDM5B-sg2	TCGAAGACCGGGCACTCGGG
KDM5B-sg3	GGACTTATTTCAGCTTAATA
KDM5C-sg1	CTTACCGCCATGACACACTT
KDM5C-sg2	GATAAACAATGCGTTCGTAG
KDM5C-sg3	GGGCTACCCGAGCCCACCGA
KDM5D-sg1	GATTTACTCCTCGCGTCCAA
KDM5D-sg2	AAAGACTTACCGCGGGTGGG
KDM5D-sg3	TAAGGCCCGACATGGAACCG

KDM6A-sg1	ACTGTAAACTGTAGTACCTC
KDM6A-sg2	CAGCATTATCTGCATACCAG
KDM6A-sg3	AGACTATGAGTCTAGTTTAA
KDM6B-sg1	TACCACAGCGCCCTTCGATA
KDM6B-sg2	ATCCCCCTCCTCGTAGCGCA
KDM6B-sg3	CAAAGGCTTCCCGTGCAGCG
PHF2-sg1	TTCTGCACGGGCTTGACGTC
PHF2-sg2	GACGTCAAGCCCGTGCAGAA
PHF2-sg3	CAGTGACGTCGAGAACTACG
PHF8-sg1	TCTGACGAACGTAGGGCTCC
PHF8-sg2	GGCTTAGTGAAAAAACGCCG
PHF8-sg3	CCTCGCCATCATTCACTGTG
BMI1-sg1	AACGTGTATTGTTCGTTACC
BMI1-sg2	TCCTACCTTATATTCAGTAG
BMI1-sg3	AAAGGTTTACCATCAGCAGA
BRD1-sg1	CACCGTGTTCTATAGAGCCG
BRD1-sg2	CGGCGCGAGGTGGACAGCAT
BRD1-sg3	CGACTCACCGGCTGCGATCC
BRD3-sg1	CGACGTGACGTTTGCAGTGA
BRD3-sg2	CAAAGGTCGGAAGCCGGCTG
BRD3-sg3	CATCACTGCAAACGTCACGT
BRD4-sg1	ACTAGCATGTCTGCGGAGAG
BRD4-sg2	TCTAGTCCATCCCCCATTAC
BRD4-sg3	GGGAACAATAAAGAAGCGCT
ING1-sg1	GAGATCGACGCGAAATACCA
ING1-sg2	TATAAATCCGCGCCCGAAAG
ING1-sg3	CCCATACCAGTTATTGCGCT
ING2-sg1	GCAGCAGCAACTGTACTCGT
ING2-sg2	GCAGCGACTCCACGCACTCA
ING2-sg3	GATCTTCAAGAAGACCCCGC
ING3-sg1	TCTCGCGCATTTCCGTGAAG
ING3-sg2	CTTCACGGAAATGCGCGAGA
ING3-sg3	TCGATACTGCATTTGTAATC
ING4-sg1	GCTGCTCGTGCTCGTTCCAA
ING4-sg2	CCTAGAAGGCCGGACTCAAA
ING4-sg3	GGCACTACTCATATACTCAG
ING5-sg1	GATCTGCTTCAAAGCGCGCC
ING5-sg2	CTTCCAGCTGATGCGAGAGC
ING5-sg3	GAAGTTCCTCTGAAGTTCGC

Dataset S2. List of PCR Primers Used in qRT-PCR

Gene Name	Primer ID	Sequence
BMI1	BMI1-F	GGCTGCTCTTTCCGGGATTT
	BMI1-R	TTGCTGGTCTCCAGGTAACG
BRD1	BRD1-F	GTCCACATCCAAGGTCAGGA
	BRD1-R	ATGGCCACCTGATTCGCAA
BRD3	BRD3-F	ACTCCAACCCCGACGAGATA
	BRD3-R	GCTTGCTGAGAACGGTTTCC
BRD4	BRD4-F	GTTGATGTGATTGCCGGCTC
	BRD4-R	TTAGGCAGGACCTGTTTCGG
CARM1	CARM1-F	TGGGCCACAACAACCTGATT
	CARM1-R	GAGGACCCTTGGACAATCCC
CREBBP	CREBBP-F	CTGCCAAGCCATCCTGGG
	CREBBP-R	GGAGTCCGAGAGCAGCATAG
DNMT1	DNMT1-F	CCATCAGGCATTCTACCAGGG
	DNMT1-R	CACCTCACAGACGCCACATC
DNMT3A	DNMT3A-F	CTGCCCAGGCAGCCATTAAG
	DNMT3A-R	TGGAGGGTCAAATTCCTGGTC
DNMT3B	DNMT3B-F	TATTGATGAGCGCACAAGAGAGC
	DNMT3B-R	GGGTGTTCCAGGGTAACATTGAG
DNMT3L	DNMT3L-F	CCGGGACAACTGAAGCATGT
	DNMT3L-R	ACAGGTACCAGCTGGGAGGA
EP300	EP300-F	CCCAAGTATGATCCGTGGCA
	EP300-R	TCCAGGTTGAGCCAACTGTC
EZH1	EZH1-F	CCCTCTCCAACAGAACTTTATGGTA
	EZH1-R	ATCATCTCTTCTTCACCATGGACT
EZH2	EZH2-F	ACATCCTTTTCATGCAACACC
	EZH2-R	GCTCCCTCCAAATGCTGGTA
GAPDH	GAPDH-F	AGCCTCAAGATCATCAGCAATG
	GAPDH-R	CAGTCTTCTGGGTGGCAGTG
HDAC1	HDAC1-F	TCAAGCCGGTCATGTCCAAA
	HDAC1-R	ACACTTGGCGTGTCCTTTGA
HDAC2	HDAC2-F	CCATAAAGCCACTGCCGAAGA
	HDAC2-R	CAGCTCCAGCAACTGAACCG
ING1	ING1-F	GGCCTAGCGCAATAACTGAGAT
	ING1-R	GATCTTCTCGTCGCCCAGC
ING2	ING2-F	ATCCTGGCTCCGCAAACG
	ING2-R	ACTCCATTTGTCTTGCCCGA
ING3	ING3-F	AAGGTTCAGTTGGCAAACCAG
	ING3-R	AGTGTCTAATTCCAAAGATCGCCT
ING4	ING4-F	TCAGCTCATGAGGGACCTAGA
	ING4-R	TGCACCTTGTCGTCACCAAA
ING5	ING5-F	GGAAAATGGTTCTGTCCACGG
	ING5-R	TTGCGACACGAATGAAGGGA
KDM1A	KDM1A-F	TCATTAGAAACCGCACACTGC
	KDM1A-R	CTCGGTGGACAAGCACAGTA
KDM1B	KDM1B-F	GCAGGCGAAGAAGAAAGCAA

	KDM1B-R	TACCATCGGGAGGTGTAGCC
KDM2A	KDM2A-F	TCCAAAGTGCTACCAGGAGG
	KDM2A-R	AGCATGGAAGTGGGTGAATGA
KDM2B	KDM2B-F	GTGGTGACTTGGCCAAAGAAG
	KDM2B-R	AAGTGGCACTCTCCGCACTC
KDM3A	KDM3A-F	TGCCAACTCTCCACCTAACC
	KDM3A-R	GAGGACTTTGAGAGCAACCCT
KDM3B	KDM3B-F	CATAGAGGGGAAAGATGGCCG
	KDM3B-R	CTGGCTCTCCACTGGCATTC
KDM4A	KDM4A-F	GCGATAAGTACTGTACCCCAC
	KDM4A-R	GCCGGCCAATATTCCACTCAT
KDM4B	KDM4B-F	TCGCATGGAGACCAAAGCCC
	KDM4B-R	GGGATGCCTCCTCGTCACTT
KDM4C	KDM4C-F	CGTACGGGTTCATGCAAGTT
	KDM4C-R	CGTTTGCTTAAGAGCACCTCC
KDM5A	KDM5A-F	CTGGCCCCCGAGTTATTTGA
	KDM5A-R	TCCTGTACACAGGCACACCA
KDM5B	KDM5B-F	CCACAAGATCCGGCCCATAG
	KDM5B-R	CACGAGTTTGGGCCTCCAAT
KDM5C	KDM5C-F	TATGCCTAAGGTCCAGGGCT
	KDM5C-R	CCTCAGGCAGTTCCAACACA
KDM5D	KDM5D-F	CTCGCGTCCAAAGGCTAAATG
	KDM5D-R	ACGATCCTTGCAGATGGCTT
KDM6A	KDM6A-F	TGACCAATTTACATTAGCTCCTCCA
	KDM6A-R	GCCAGCAGCCTTACGAGATA
KDM6B	KDM6B-F	CCCCTCACCGCCTATCAGTA
	KDM6B-R	TCTTGAACAAGTCGGGGTCG
MBD1	MBD1-F	TGGTGCCAAACTGGCTACT
	MBD1-R	GTGTCTGAGCGTCCACAGG
MBD2	MBD2-F	ACGAATGAATGAACAGCCACG
	MBD2-R	TGGACCAACTCCTTGAAGACC
MLL	MLL-F	CGACAGCAAGGGCATTGGTT
	MLL-R	AGTGAGTTCCTCTCCTCGGT
MLL2	MLL2_F	TGTGGGTCCTGTGTCAACTG
	MLL2-R	TTCACTATCGTCCGGCCTTT
NSD1	NSD1-F	AGCGCCAATATCCAGAGGTT
	NSD1-R	ATACTCATTCACAAATTCACCCTTT
PHF2	PHF2-F	GCCTCTAACCACAGCGAGAT
	PHF2-R	AGATCCAGCCTGAGGGGATG
PHF8	PHF8-F	ATACCAGACTTTCTAACCTTGTGGA
	PHF8-R	CGCACACTCATGAGGCAGTA
PRMT1	PRMT1-F	GCAAGGTCATCGGGATCGAG
	PRMT1-R	GGTGTTGAGCATGGACTCGT
PRMT2	PRMT2-F	GGCAGCTATGGAACTCTGAAAC
	PRMT2-R	CCCACGTCCAGGATGACTTT
PRMT3	PRMT3-F	ACCCCAATGGACTCAGTGAA
	PRMT3-R	CAAAATCCTGAGCAAATTGTTTCAT
PRMT5	PRMT5-F	TATCTGCAGTCCCCGCTTCA

	PRMT5-R	TAGATGGCCTGCTGGTACTG
PRMT6	PRMT6-F	AAGATGTCGCAGCCCAAGAA
	PRMT6-R	GGACCGAAACGTCCGAGTAG
PRMT7	PRMT7-F	ACTACCAAGGTATCCGGGCT
	PRMT7-R	GGCTTGAAAACCTCGATGGC
SETD2	SETD2-F	TAATCTCTTGGATCTGCCGCC
	SETD2-R	CCCACTGAGTCTGCCTTGTG
SIRT1	SIRT1-F	TAATCAGGTAGTTCCTCGATGTCC
	SIRT1-R	AGGAGGTCAACTTCATCTTTGTCA

Dataset S3. Sequencing of Targeted Alleles in OVCAR8-ADR-Cas9 Single Cells Harboring BMI1-sg2 and PHF8-sg2 Expression Construct
(Please refer to Supplementary Excel file)

Dataset S4. List of Two-Wise gRNA Hits that Inhibit OVCAR8-ADR Cell Proliferation Based on Pooled Screening

sgRNA-A	sgRNA-B	Log_2 ratio – Day 20/Day15 (Replicate 1)	Log_2 ratio – Day 20/Day15 (Replicate 2)	Q-value
BRD4_sg3	MLL_sg3	-2.61	-3.32	7.01E-33
BMI1_sg2	HDAC2_sg3	-3.91	-1.93	3.41E-32
BMI1_sg2	KDM1B_sg3	-1.34	-3.71	1.20E-23
ING3_sg3	BMI1_sg1	-3.68	-1.11	4.57E-21
BRD4_sg3	KDM6A_sg2	-2.30	-2.20	1.52E-18
BRD4_sg3	PHF2_sg2	-1.57	-2.88	4.05E-18
BMI1_sg2	PRMT6_sg1	-2.80	-1.59	1.19E-17
ING3_sg2	KDM5A_sg2	-2.28	-2.04	3.48E-17
KDM5B_sg3	MLL_sg3	-3.17	-1.05	2.61E-16
KDM6A_sg3	KDM6A_sg2	-1.95	-2.26	2.61E-16
BRD4_sg3	KDM4C_sg1	-1.48	-2.28	7.88E-13
KDM6B_sg1	KDM3A_sg2	-0.98	-2.70	3.00E-12
ING3_sg3	KDM6A_sg2	-1.46	-2.10	2.02E-11
PRMT5_sg3	PRMT5_sg3	-1.54	-1.92	9.13E-11
BRD4_sg3	BRD4_sg2	-2.45	-1.00	1.24E-10
BMI1_sg2	NSD1_sg3	-2.19	-1.20	2.68E-10
BMI1_sg2	MBD2_sg3	-1.44	-1.93	3.94E-10
BMI1_sg2	KDM1A_sg1	-1.62	-1.40	5.85E-08
KDM3A_sg2	PRMT5_sg3	-1.28	-1.72	6.62E-08
BRD4_sg3	EP300_sg3	-1.28	-1.71	7.28E-08
BMI1_sg2	KDM3A_sg1	-1.47	-1.48	1.32E-07
BRD4_sg3	KDM6B_sg1	-1.20	-1.64	5.58E-07
PHF8_sg2	KDM1A_sg1	-1.11	-1.69	8.77E-07
KDM6A_sg3	HDAC2_sg3	-1.03	-1.77	8.77E-07
BRD4_sg3	KDM6B_sg2	-0.92	-1.86	1.13E-06
PRMT5_sg3	HDAC1_sg1	-1.26	-1.43	3.14E-06
PHF8_sg2	PRMT5_sg3	-1.60	-1.08	3.50E-06
BRD4_sg3	PHF2_sg1	-1.51	-1.13	5.35E-06
BRD4_sg3	EZH2_sg3	-1.02	-1.57	8.80E-06
PRMT5_sg3	EZH1_sg1	-0.96	-1.62	9.53E-06
KDM6A_sg2	KDM5A_sg2	-1.48	-1.04	1.72E-05
BRD4_sg3	KDM2B_sg2	-1.00	-1.49	2.59E-05
KDM6B_sg3	PRMT5_sg3	-1.03	-1.43	3.60E-05
BRD4_sg1	KDM6B_sg1	-1.30	-1.15	3.74E-05
KDM1A_sg3	PRMT5_sg3	-1.52	-0.91	4.81E-05
PRMT5_sg3	EP300_sg2	-1.41	-1.00	5.44E-05
BRD4_sg3	PRMT5_sg2	-1.46	-0.91	7.59E-05

KDM5D_sg2	MLL_sg3	-1.01	-1.34	9.28E-05
BRD4_sg3	PRMT5_sg3	-1.03	-1.33	9.28E-05
PHF2_sg1	PRMT5_sg3	-1.19	-1.13	1.32E-04
PRMT5_sg2	DNMT1_sg1	-1.28	-1.02	1.54E-04
KDM6A_sg2	KDM5C_sg1	-1.28	-1.01	1.73E-04
BMI1_sg2	KDM6A_sg2	-0.96	-1.30	2.47E-04
KDM1A_sg1	PRMT5_sg3	-0.95	-1.29	2.68E-04
BRD4_sg2	KDM2B_sg1	-1.06	-1.17	2.82E-04
KDM4A_sg2	PRMT5_sg3	-1.07	-1.16	3.18E-04
PRMT6_sg2	PRMT5_sg2	-1.02	-1.13	6.20E-04
KDM2B_sg3	PRMT5_sg3	-1.13	-1.01	6.95E-04
KDM6B_sg1	MLL_sg3	-0.92	-1.19	9.39E-04
BRD4_sg3	BMI1_sg2	-0.94	-1.14	1.10E-03
KDM5A_sg3	NSD1_sg3	-0.91	-1.14	1.37E-03
BRD4_sg3	KDM3A_sg2	-0.92	-1.13	1.37E-03
KDM6B_sg3	PRMT7_sg3	-1.11	-0.90	1.85E-03
BRD3_sg3	KDM4C_sg1	-0.99	-1.01	2.13E-03
KDM4C_sg1	PRMT5_sg3	-0.93	-1.06	2.15E-03
KDM3B_sg1	PRMT5_sg3	-1.00	-0.99	2.15E-03
PRMT5_sg2	MBD1_sg1	-0.94	-1.04	2.47E-03
EP300_sg3	MBD1_sg3	-0.92	-1.03	2.93E-03
ING3_sg1	BRD4_sg3	-0.99	-0.96	2.93E-03
KDM1A_sg1	HDAC2_sg3	-0.94	-0.95	4.71E-03
PRMT5_sg2	CARM1_sg1	-0.95	-0.91	5.78E-03

Dataset S5. Constructs Used in This Work

Construct ID	Design
pAWp28	pBT264-U6p-{2xBbsI}-sgRNA scaffold-{MfeI}
pAWp28-1	pBT264-U6p-GFP-sg1
pAWp28-2	pBT264-U6p-RFP-sg1
pAWp28-3	pBT264-U6p-RFP-sg2
pAWp28-4	pBT264-U6p-KDM4C-sg1
pAWp28-5	pBT264-U6p-PHF2-sg1
pAWp28-6	pBT264-U6p-KDM6B-sg2
pAWp28-7	pBT264-U6p-PHF2-sg2
pAWp28-8	pBT264-U6p-DNMT1-sg1
pAWp28-9	pBT264-U6p-DNMT3B-sg1
pAWp28-10	pBT264-U6p-PRMT2-sg3
pAWp28-11	pBT264-U6p-HDAC2-sg1
pAWp28-12	pBT264-U6p-ING4-sg1
pAWp28-13	pBT264-U6p-KDM1B-sg3
pAWp28-14	pBT264-U6p-KDM2A-sg3
pAWp28-15	pBT264-U6p-PRMT6-sg1
pAWp28-16	pBT264-U6p-BMI1-sg2
pAWp28-17	pBT264-U6p-PHF8-sg2
pAWp28-18	pBT264-U6p-BRD4-sg2
pAWp28-19	pBT264-U6p-BRD4-sg3
pAWp28-20	pBT264-U6p-KDM6A-sg2
pAWp28-21	pBT264-U6p-KDM6A-sg3
pAWp28-22	pBT264-U6p-NF1-sg1
pAWp28-23	pBT264-U6p-NF1-sg4
pAWp28-24	pBT264-U6p-NF2-sg2
pAWp28-25	pBT264-U6p-MED12-sg1
pAWp9	pFUGW-UBCp-*RFP*-CMVp-*GFP*-{BamHI+EcoRI}
pAWp9-1	pFUGW-UBCp-*RFP*-CMVp-*GFP*-U6p-GFP-sg1
pAWp9-2	pFUGW-UBCp-*RFP*-CMVp-*GFP*-U6p-RFP-sg1
pAWp9-3	pFUGW-UBCp-*RFP*-CMVp-*GFP*-U6p-RFP-sg2
pAWp9-4	pFUGW-UBCp-*RFP*-CMVp-*GFP*-U6p-RFP-sg1-U6p-GFP-sg1
pAWp9-5	pFUGW-UBCp-*RFP*-CMVp-*GFP*-U6p-RFP-sg2-U6p-GFP-sg1
pAWp11	pFUGW-CMVp
pAWp12	pFUGW-CMVp-*GFP*
pAWp12-1	pFUGW-CMVp-*GFP*-[U6p-BRD4-sg3]-[U6p-PHF2-sg1]
pAWp12-2	pFUGW-CMVp-*GFP*-[U6p-BRD4-sg3]-[U6p-KDM6B-sg2]
pAWp12-3	pFUGW-CMVp-*GFP*-[U6p-BRD4-sg3]-[U6p-KDM4C-sg1]
pAWp12-4	pFUGW-CMVp-*GFP*-[U6p-BRD4-sg3]-[U6p-PHF2-sg2]
pAWp12-5	pFUGW-CMVp-*GFP*-[U6p-BRD4-sg3]

pAWp12-6	pFUGW-CMVp-*GFP*-[U6p-KDM4C-sg1]
pAWp12-7	pFUGW-CMVp-*GFP*-[U6p-KDM6B-sg2]
pAWp12-8	pFUGW-CMVp-*GFP*-[U6p-DNMT1-sg1]
pAWp12-9	pFUGW-CMVp-*GFP*-[U6p-DNMT3B-sg1]
pAWp12-10	pFUGW-CMVp-*GFP*-[U6p-PRMT2-sg3]
pAWp12-11	pFUGW-CMVp-*GFP*-[U6p-HDAC2-sg1]
pAWp12-12	pFUGW-CMVp-*GFP*-[U6p-ING4-sg1]
pAWp12-13	pFUGW-CMVp-*GFP*-[U6p-KDM1B-sg3]
pAWp12-14	pFUGW-CMVp-*GFP*-[U6p-KDM2A-sg3]
pAWp12-15	pFUGW-CMVp-*GFP*-[U6p-PRMT6-sg1]
pAWp12-16	pFUGW-CMVp-*GFP*-[U6p-BMI1-sg2]-[U6p-PHF8-sg2]
pAWp12-17	pFUGW-CMVp-*GFP*-[U6p-BRD4-sg2]-[U6p-KDM4C-sg1]
pAWp12-18	pFUGW-CMVp-*GFP*-[U6p-BRD4-sg3]-[U6p-BRD4-sg2]
pAWp12-19	pFUGW-CMVp-*GFP*-[U6p-KDM6A-sg3]-[U6p-KDM6A-sg2]
pAWp12-20	pFUGW-CMVp-*GFP*-[U6p-KDM6A-sg2]
pAWp12-21	pFUGW-CMVp-*GFP*-[U6p-KDM6A-sg3]
pAWp12-22	pFUGW-CMVp-*GFP*-[U6p-BRD4-sg2]
pAWp12-23	pFUGW-CMVp-*GFP*-[U6p-BMI1-sg2]
pAWp12-24	pFUGW-CMVp-*GFP*-[U6p-PHF8-sg2]
pAWp12-25	pFUGW-CMVp-*GFP*-[U6p-PHF2-sg1]
pAWp12-26	pFUGW-CMVp-*GFP*-[U6p-PHF2-sg2]
pAWp12-27	pFUGW-CMVp-*GFP*-[U6p-NF1-sg1]
pAWp12-28	pFUGW-CMVp-*GFP*-[U6p-NF1-sg4]
pAWp12-29	pFUGW-CMVp-*GFP*-[U6p-NF2-sg2]
pAWp12-30	pFUGW-CMVp-*GFP*-[U6p-MED12-sg1]
pAWp21	pLKO.1-Control sh
pAWp21-1	pLKO.1-KDM4C-sh1
pAWp21-2	pLKO.1-KDM4C-sh2
pAWp21-3	pLKO.1-KDM6B-sh
pAWp21-4	pLKO.1-BRD4-sh1
pAWp21-5	pLKO.1-BRD4-sh2
pAWp30	pFUGW-EFSp-*Cas9-P2A-Zeo*

Dataset S6. shRNA Antisense Sequences Used for Individual Validation Assay

shRNA ID	shRNA antisense sequence
Control-sh	CGAGGGCGACTTAACCTTAGG
KDM4C-sh1	AAATCTTCGTAATCCAAGTAT
KDM4C-sh2	GTAATACCGGGTGTTCCGATG
KDM6B-sh	ATTAATCCACACGAGGTCTCC
BRD4-sh1	TATAGTAATCAGGGAGGTTCA
BRD4-sh2	TTTAGACTTGATTGTGCTCAT

Dataset S7. Barcode Counts for the Pooled Screen
(Please refer to Supplementary Excel file)

Dataset S8. Log_2 Ratios Determined for Two-Wise gRNA Combinations Based on Pooled Screening
(Please refer to Supplementary Excel file)

Dataset S9. List of PCR Primers Used in Surveyor Assay and Sanger Sequencing for Genome Modification Detection

Target sgRNA ID	Forward primer (5' to 3')	Reverse primer (5' to 3')
BMI1-sg2	AGAAATTAAACGGCTACCCTCCA	GTTGGTACAAAGTGGTGAAGGC
BRD4-sg2	TCCATAGTGTCTTGAGCACCAC	ACGTGGCTTCATTGTACATCCT
BRD4-sg3	CACTTGCTGATGCCAGTAGGAG	AAGCACATGCTTCAGGCTAACA
DNMT1-sg1	GTGAATAGCTTGGGAATGTGGG	TCATCTGCTCTTACGCTTAGCC
DNMT3B-sg1	GCCACACTCTACATGGGAGC	CTCGGCAACCCTCCATACAT
HDAC2-sg1	GACTTTTCCATCAGGGACACCT	AACCATGCACAGAATCCAGATTTA
ING4-sg1	GGTGGACAAACACATTCGGC	AAGAGTTCTTGGCGCAGACA
KDM1B-sg3	CCTATCATTGCCCCAAGGAGTC	TCGTCCAAGTTACAGTCATCACA
KDM2A-sg3	CTAGGCCTCCGACAGTTGTAAT	TCCTCTGGTGCACAGAAAAGTC
KDM4C-sg1	AGCCACCCTTGGTTGGTTTT	TTCTCTCCAGACACTGCCCT
KDM6B-sg2	GGTAAGGGAAACTCTGGGGC	GTGCCCAGAACTACTGCCAT
PHF8-sg2	CTCCCTCCCTTCCTAAGGCT	GAGGTGAGTTCCAGCTTCCC
PRMT2-sg3	ATTGCCTTAAGTCGACACCTGAT	CACCTTACAGGCACTGCGTT
PRMT6-sg1	GACTGTAGAGTTGCCGGAACAG	CTCCCTCCCTAGAGGCTATGAG

Dataset S10. List of PCR Primers Used in Deep Sequencing for Indel Detection

Target gRNA ID	Type of target site	20 bp gRNA targeting sequence (5' to 3')	Forward primer (5' to 3')	Reverse primer (5' to 3')
NF1-sg1	On-target	GTTGTGCTCAGTACTGACTT	ACACTCTTTCCCTACACGACGCTCTTCCGATCT-GGTATCTGTGGTTGATGCAGTTTTCC	GTGACTGGAGTTCAGACGTGTGCTCTTCCGATCT-AGTAGTGAGGCCGCTTATAACC
NF1-sg4	On-target	TTTCAGCTTCCAATAAAAAC	ACACTCTTTCCCTACACGACGCTCTTCCGATCT-GGTATCTGTGGTTGATGCAGTTTTCC	GTGACTGGAGTTCAGACGTGTGCTCTTCCGATCT-AGTAGTGAGGCCGCTTATAACC
NF2-sg2	On-target	ATTCCACGGGAAGGAGATCT	ACACTCTTTCCCTACACGACGCTCTTCCGATCT-GCACAGAGCTGCTGCTTGGAGTG	GTGACTGGAGTTCAGACGTGTGCTCTTCCGATCT-TAACAAGGAGATGCCCTGGCTGG
MED12-sg1	On-target	AGGATTGAAGCTGACGTTCT	ACACTCTTTCCCTACACGACGCTCTTCCGATCT-CGCTTTCCTGCCTCAGGATGAAC	GTGACTGGAGTTCAGACGTGTGCTCTTCCGATCT-AGGTCATGAAGGCAAACTCAGCC
PHF8-sg2	On-target	GGCTTAGTGAAAAAACGCCG	ACACTCTTTCCCTACACGACGCTCTTCCGATCT-TTGGAAGAGAAGGATCTGCTGAGGC	GTGACTGGAGTTCAGACGTGTGCTCTTCCGATCT-CACCTGTCAAAAGTCCTACTCCGG
BMI-sg2	On-target	TCCTACCTTATATTCAGTAG	ACACTCTTTCCCTACACGACGCTCTTCCGATCT-GCTACCCTCCACAAAGCACACAC	GTGACTGGAGTTCAGACGTGTGCTCTTCCGATCT-CCTGGAGACCAGCAAGTATTGTCC
KDM4C-sg1	On-target	CCTTTGCAAGACCCGCACGA	ACACTCTTTCCCTACACGACGCTCTTCCGATCT-CCTTCAGAAACAATGTCCCAAATCG	GTGACTGGAGTTCAGACGTGTGCTCTTCCGATCT-GTCCTCTGAACCCCAGCTGTAAG
KDM4C-sg1	Off-target	GCTTTGCCCGAACCGCACGA	ACACTCTTTCCCTACACGACGCTCTTCCGATCT-AGCCTTTCTGAGAGCGGGCTAG	GTGACTGGAGTTCAGACGTGTGCTCTTCCGATCT-CAAACAGAGGCCAAAGGGTGTCCC
KDM4C-sg1	Off-target	CCTAGGCCAGACCTGCACGA	ACACTCTTTCCCTACACGACGCTCTTCCGATCT-GCCTCCTCTCATCCTCTCGCTTC	GTGACTGGAGTTCAGACGTGTGCTCTTCCGATCT-ACAGGAGGTCGTGGTGCAGTTCTC
KDM4C-sg1	Off-target	GCTCTGGAAGACCCGCACCA	ACACTCTTTCCCTACACGACGCTCTTCCGATCT-GATTGGCTCCAAGCGGCCATCAAAC	GTGACTGGAGTTCAGACGTGTGCTCTTCCGATCT-TTGTGTGAGGAACGTTGACGCTACC
KDM4C-sg1	Off-target	CCTTATCAAGACCCACACCA	ACACTCTTTCCCTACACGACGCTCTTCCGATCT-TTGAACTCAAGGCTCAGCCAACAGGC	GTGACTGGAGTTCAGACGTGTGCTCTTCCGATCT-GAGCGTAGGTCCTCTGCATGGAG

KDM6B-sg2	On-target	ATCCCCCTCCTCGTAGCGCA	ACACTCTTTCCCTACACGACGCTCTTCCGATCT-CAACTCAGGCTGGATGCATCGG	GTGACTGGAGTTCAGACGTGTGCTCTTCCGATCT-CCACAGAATGACAGGAACCCATGG
KDM6B-sg2	Off-target	CTGCTCCTCCTCGTAGCGCT	ACACTCTTTCCCTACACGACGCTCTTCCGATCT-TTGGTGGCCGCTGAGTGTGTGTAC	GTGACTGGAGTTCAGACGTGTGCTCTTCCGATCT-ACTGAGCAGAGCCTAGGAGGCAG
KDM6B-sg2	Off-target	TGCGCCCTCCTCCTAGCGCA	ACACTCTTTCCCTACACGACGCTCTTCCGATCT-CAGCATGTTGACATAGCGGC	GTGACTGGAGTTCAGACGTGTGCTCTTCCGATCT-TGTTGCCAGATCCAGAGGCGTC
KDM6B-sg2	Off-target	CTCCTCCTCCGCGTAGCGCT	ACACTCTTTCCCTACACGACGCTCTTCCGATCT-TGAGAGGAGATGAGTCGGGGTC	GTGACTGGAGTTCAGACGTGTGCTCTTCCGATCT-AACTGGCCCGAGTAGTCGGAGCAG
KDM6B-sg2	Off-target	CTGCCCCTCCTGGTAGCGCC	ACACTCTTTCCCTACACGACGCTCTTCCGATCT-GACGGGTCAAAGCCTCAGGAGAG	GTGACTGGAGTTCAGACGTGTGCTCTTCCGATCT-TCCTCAGAGTGTGTGGAAGTGCTGG
KDM6B-sg2	Off-target	AACCAGCTCCTCGTAGCTCA	ACACTCTTTCCCTACACGACGCTCTTCCGATCT-TTAGCTGCCCAGCTCACAGCTACC	GTGACTGGAGTTCAGACGTGTGCTCTTCCGATCT-AAGAGCTCCTAGGGGAGGATCAG
KDM6B-sg2	Off-target	ACCGCCCTCCTCCTAGCTCA	ACACTCTTTCCCTACACGACGCTCTTCCGATCT-GAGCCCCAAGAGCGAGACAA	GTGACTGGAGTTCAGACGTGTGCTCTTCCGATCT-TGGCAGGAGCACAGCCTAAGGA
KDM6B-sg2	Off-target	AGCCCGCTCCTCGTGGGGCA	ACACTCTTTCCCTACACGACGCTCTTCCGATCT-GGCGCTCAGAAGGCTGTGCAG	GTGACTGGAGTTCAGACGTGTGCTCTTCCGATCT-ACACCCGCCTCGGAGATCAACAC
BRD4-sg3	On-target	GGGAACAATAAAGAAGCGCT	ACACTCTTTCCCTACACGACGCTCTTCCGATCT-CCTAGGTGACACTGGACTTTTGC	GTGACTGGAGTTCAGACGTGTGCTCTTCCGATCT-CCACCCCTACATCTCACCTTGTTG
BRD4-sg3	Off-target	TGGAAAAACAAAGAAGAGCT	ACACTCTTTCCCTACACGACGCTCTTCCGATCT-AGGTTCACCTCAGGCTGCTCAGAAG	GTGACTGGAGTTCAGACGTGTGCTCTTCCGATCT-GTGAGGTTTCCACGTGCCAGC
BRD4-sg3	Off-target	GGGAAGTATAAGGAAGAGCT	ACACTCTTTCCCTACACGACGCTCTTCCGATCT-CGTCTCTCTCCATGTGAGCTTGTG	GTGACTGGAGTTCAGACGTGTGCTCTTCCGATCT-CCAACAATTCCAGGTATGAAACTCCC
BRD4-sg3	Off-target	GTGAGCAATAAAGCAGCCCT	ACACTCTTTCCCTACACGACGCTCTTCCGATCT-GGAAAGATCATCTGATCAGGCCCATC	GTGACTGGAGTTCAGACGTGTGCTCTTCCGATCT-CTCCCCACTTGTAGGTTCCTAATCC
BRD4-sg2	On-target	TCTAGTCCATCCCCCATTAC	ACACTCTTTCCCTACACGACGCTCTTCCGATCT-	GTGACTGGAGTTCAGACGTGTGCTCTTCCGATCT-

			CTTGTTAGGGTTGGAGG TCTCTGG	GTAGAGTGCCTGGTGAA GAATGTG
BRD4-sg2	Off-target	AATATTCCATT CCCCATTAC	ACACTCTTTCCCTACAC GACGCTCTTCCGATCT-AAGGCCCGTAAAGGGC AAGTTCAG	GTGACTGGAGTTCAGAC GTGTGCTCTTCCGATCT-TCCAGACTGTTGTTCAG TCCTGT
BRD4-sg2	Off-target	TGTTGTCCATA CCTCATTAC	ACACTCTTTCCCTACAC GACGCTCTTCCGATCT-GGTGACAGGAAGCTGTC GGAACAT	GTGACTGGAGTTCAGAC GTGTGCTCTTCCGATCT-CTCTGGATTTGCCCACA CCTAGTC
BRD4-sg2	Off-target	TCTAGGTCATG CACCATTAC	ACACTCTTTCCCTACAC GACGCTCTTCCGATCT-CTCACTGTGATCTGACA CCAAACAC	GTGACTGGAGTTCAGAC GTGTGCTCTTCCGATCT-GCATGCTTGCTTTCTGA AGGTGGC
BRD4-sg2	Off-target	CCCATTCCTTC CCCCATTAC	ACACTCTTTCCCTACAC GACGCTCTTCCGATCT-CTAGTTGCCTTCATGCCT TACAGAC	GTGACTGGAGTTCAGAC GTGTGCTCTTCCGATCT-TTCCAAGCAAGTGAGCT TCAGCACC
BRD4-sg2	Off-target	TCCACACCCTC CCCCATTAC	ACACTCTTTCCCTACAC GACGCTCTTCCGATCT-CTGCTCCCACTCCAGAC TACCC	GTGACTGGAGTTCAGAC GTGTGCTCTTCCGATCT-CCACCCATGACACAGGA GGG

Dataset S11. List of PCR Primers Used in Whole Genome Amplification for Indel Detection

Target sgRNA ID	Forward primer (5' to 3')	Reverse primer (5' to 3')
BMI1-sg2	GTCTCGTGGGCTCGGAGATGTGTATAAGAGACAGGCTACCCTCCACAAAGCACACAC	TCGTCGGCAGCGTCAGATGTGTATAAGAGACAGCCTGGAGACCAGCAAGTATTGTCC
PHF8-sg2	GTCTCGTGGGCTCGGAGATGTGTATAAGAGACAGTTGGAAGAGAAGGATCTGCTGAGGC	TCGTCGGCAGCGTCAGATGTGTATAAGAGACAGCACCTGTCAAAAGTCCTACTCCGG

Supporting Information References

1. Moffat J, et al. (2006) A Lentiviral RNAi Library for Human and Mouse Genes Applied to an Arrayed Viral High-Content Screen. *Cell* 124:1283–1298.

2. Shalem O, et al. (2014) Genome-scale CRISPR-Cas9 knockout screening in human cells. *Science* 343:84–7.

3. Bassik MC, et al. (2013) A systematic mammalian genetic interaction map reveals pathways underlying ricin susceptibility. *Cell* 152:909–922.

4. Storey JD, Tibshirani R (2003) Statistical significance for genomewide studies. *Proc Natl Acad Sci U S A* 100:9440–9445.

5. Bliss CI (1939) The toxicity of poisons applied jointly. *Ann Appl Biol* 26:585–615.

6. Borisy AA, et al. (2003) Systematic discovery of multicomponent therapeutics. *Proc Natl Acad Sci U S A* 100:7977–7982.

7. Wong ASL, Choi GCG, Cheng AA, Purcell O, Lu TK (2015) Massively parallel high-order combinatorial genetics in human cells. *Nat Biotechnol* 33:952–961.

8. Ran FA, et al. (2013) Genome engineering using the CRISPR-Cas9 system. *Nat Protoc* 8:2281–308.

9. Stemmer M (2015) CCTop: An Intuitive, Flexible and Reliable CRISPR/Cas9 Target Prediction Tool. *PLoS One* 10(4):e0124633.

10. Kim D, et al. (2013) TopHat2: accurate alignment of transcriptomes in the presence of insertions, deletions and gene fusions. *Genome Biol* 14:R36.

11. Langmead B, Trapnell C, Pop M, Salzberg SL (2009) Ultrafast and memory-efficient alignment of short DNA sequences to the human genome. *Genome Biol* 10:R25.

12. Trapnell C, et al. (2013) Differential analysis of gene regulation at transcript resolution with RNA-seq. *Nat Biotechnol* 31:46–53.

13. Subramanian A, et al. (2005) Gene set enrichment analysis: a knowledge-based approach for interpreting genome-wide expression profiles. *Proc Natl Acad Sci U S A* 102:15545–50.